iScience

CellPress
OPEN ACCESS

Article

# Suppression of preadipocyte determination by SOX4 limits white adipocyte hyperplasia in obesity

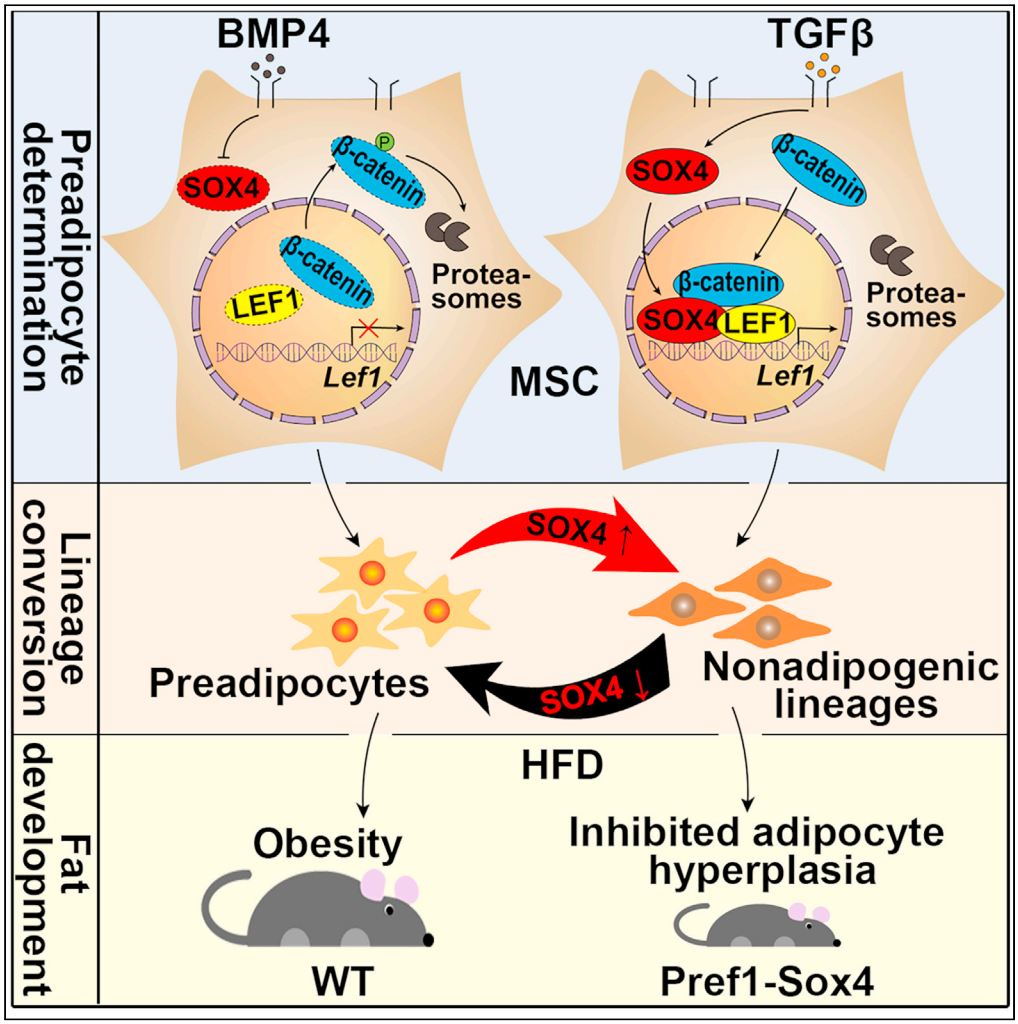


Ting He, Shuai Wang, Shengnan Li, ..., Rui Zhang, Dongyan Shen, Boan Li

raissarui@foxmail.com (R.Z.)
shendongyan@163.com (D.S.)
bali@xmu.edu.cn (B.L.)

## Highlights

SOX4 transmits BMP- and TGFβ-signaling and inhibits preadipocyte determination

SOX4 promotes adipogenic-nonadipogenic lineage conversion

SOX4 cooperates with LEF1 to activate the Wnt targets and inhibit preadipocyte genes

Preadipocyte-specific SOX4 overexpression inhibits adipocyte hyperplasia and obesity

He et al., iScience 26, 106289
April 21, 2023 
https://doi.org/10.1016/j.isci.2023.106289

iScience

CellPress
OPEN ACCESS

Article

# Suppression of preadipocyte determination by SOX4 limits white adipocyte hyperplasia in obesity

Ting He,[1,5] Shuai Wang,[1,5] Shengnan Li,[1,3,5] Huanming Shen,[1,5] Lingfeng Hou,[1] Yunjia Liu,[1] Yixin Wei,[1] Fuan Xie,[4] Zhiming Zhang,[2] Zehang Zhao,[1] Chunli Mo,[1] Huiling Guo,[1] Qingsong Huang,[1] Rui Zhang,[2,*] Dongyan Shen,[2,*] and Boan Li[1,6,*]

## SUMMARY

**Preadipocyte determination expanding the pool of preadipocytes is a vital process in adipocyte hyperplasia, but the molecular mechanisms underlying this process are yet to be elucidated. Herein, SRY-related HMG box transcription factor 4 (SOX4) was identified as a critical target in response to BMP4- and TGFβ-regulated preadipocyte determination. SOX4 deficiency is sufficient to promote preadipocyte determination in mesenchymal stem cells (MSCs) and acquisition of preadipocyte properties in nonadipogenic lineages, while its overexpression impairs the adipogenic capacity of preadipocytes and converts them into nonadipogenic lineages. Mechanism studies indicated that SOX4 activates and cooperates with LEF1 to retain the nuclear localization of β-catenin, thus mediating the crosstalk between TGFβ/BMP4 signaling pathway and Wnt signaling pathway to regulate the preadipocyte determination. *In vivo* studies demonstrated that SOX4 promotes the adipogenic-nonadipogenic conversion and suppresses the adipocyte hyperplasia. Together, our findings highlight the importance of SOX4 in regulating the adipocyte hyperplasia in obesity.**

## INTRODUCTION

Obesity prevalence has attracted widespread attention due to its strong association with shortened life expectancy, metabolic diseases, cardiovascular diseases, and even tumorigenesis.[1,2] Adipocyte hyperplasia is a major character of obesity. It occurs to increase the capacity for energy storage and adaption to the changes in metabolic levels.[3,4] Adipocyte hyperplasia is initiated by the recruitment of pluripotent mesenchymal stem cells (MSCs),[5] a cell population that resides in the vascular stroma of white adipose tissues (WATs) with the potential to differentiate into adipocytes, myocytes, osteocytes, and chondrocytes. In response to some specific signals, these pluripotent MSCs undergo preadipocyte determination and transform into preadipocytes with high adipogenic capacity, followed by rapid adipocyte differentiation.[6] A potential feature in diabetic subjects is that a smaller preadipocyte pool limits the generation of new adipocytes.[7] Thus, understanding the process of preadipocyte determination is crucial for regulating the adipocyte hyperplasia in obesity and developing therapeutic approaches against obesity-associated metabolic diseases. However, the intrinsic signals to control preadipocyte determination are yet in the nascent stage.

In previous studies, several extracellular signals have been shown to regulate preadipocyte determination. Transforming growth factor β (TGFβ) signaling plays a critical role in augmenting the proliferation of adipose tissue-derived MSCs and inhibiting their preadipocyte determination.[8] TGFβ cytokine also triggers the development of mesenchymal marrow stem cells toward osteoblasts rather than preadipocytes.[9] Bone marrow adipogenesis with TGFβ signaling is attenuated during aging.[9] BMP4, another signaling molecule of TGFβ superfamily, plays a dominant role in triggering the fate determination of both embryonic fibroblasts and MSCs toward adipocyte lineages.[10–13] The treatment of multipotent MSCs with BMP4 protein during proliferation activates both SMAD1/$^{5}/_{8}$ and p38 MAPK and generates a population of preadipocyte-like cells that subsequently enter the adipocyte differentiation pathways and acquire adipocyte phenotypes.[11,12] These studies suggested that the extracellular TGFβ and BMP4 signals play an antagonistic role in preadipocyte determination. However, the potential mediators and the underlying molecular mechanisms are yet to be revealed.

[1]State Key Laboratory of Cellular Stress Biology, Innovation Center for Cell Signaling Network and Engineering Research Center of Molecular Diagnostics of The Ministry of Education, School of Life Sciences, Xiamen University, Xiamen, Fujian 361100, China

[2]Xiamen Cell Therapy Research Center, the First Affiliated Hospital of Xiamen University, School of Medicine, Xiamen University, Xiamen, Fujian 361003, China

[3]School of Medicine, Henan Polytechnic University, Jiaozuo, Henan 454000, China

[4]Xiamen University Research Center of Retroperitoneal, Tumor Committee of Oncology Society of Chinese Medical Association, Xiang'an Hospital of Xiamen University, School of Medicine, Xiamen University, Xiamen, Fujian 361102, China

[5]These authors contributed equally

[6]Lead contact

*Correspondence: raissarui@foxmail.com (R.Z.), shendongyan@163.com (D.S.), bali@xmu.edu.cn (B.L.)

https://doi.org/10.1016/j.isci.2023.106289

Wnt/β-catenin signaling pathway is involved in the inhibition of both preadipocyte determination and the early stage of adipocyte differentiation. β-Catenin is the central signaling molecule of the Wnt/β-catenin pathway. Its nucleocytoplasmic shuttling and subcellular localization determine the transduction of Wnt signal. TCF4 and BCL9/Pygopus recruit β-catenin to the nucleus to activate the target genes, while APC, AXIN, and AXIN2 enrich the molecule in the cytoplasm to target its phosphorylation and degradation.[14] Some studies demonstrated that genetic variations/mutations in the Wnt/β-catenin pathway are associated with human obesity and metabolic diseases.[15–19] These findings could be attributed to the ability of Wnt signaling to inhibit adipocyte differentiation and maintain the committed preadipocyte in an undifferentiated state.[6,20,21] Emerging evidence suggested that Wnt/β-catenin signaling inhibits preadipocyte determination during the early stage of fat development. Zeve et al. observed that the overexpression of β-catenin in mesenchymal progenitors disrupts adipose tissue development and induces a fate change toward fibroblasts.[22] Nonetheless, how the Wnt signaling pathway is regulated during this process remains largely unknown, and the key transcription factor responsible for signaling transduction and target activation is yet to be identified.

SRY-related HMG box transcription factor 4 (SOX4) is a SOXC group transcription factor with a preference for the A/T A/T CAAA T/G motif, which plays a key architectural role in the assembly of transcriptional enhancer complexes to activate the transcription of target genes.[23,24] During embryonic development, SOX4 is highly expressed in mesenchymal tissues and plays a critical role in the development and differentiation of multiple tissues by maintaining their precursor cells in an undifferentiated state.[25–27] In adult individuals, SOX4 expression might be limited to specific tissues and cell types with vigorous division.[28–31] In cancer cells, SOX4 is a central component of TGFβ-induced epithelial-mesenchymal transition.[32] In addition, TGFβ-activated Smad2/3 complex binds to the *Sox4* promoter and recruits chromatin-modifier enzymes, thereby stimulating the expression of SOX4.[33,34] Whether SOX4 has a role in fat development remains to be clarified.

Herein, we revealed that SOX4 inhibits preadipocyte determination and initiates adipogenic-nonadipogenic conversion in the early stage of fat development. It functions in transmitting the antagonistic signals of BMP4 and TGFβ signaling pathways in MSCs. Subsequently, SOX4 promotes the transcription of *Lef1*, which in turn cooperates with SOX4 to bind the adjacent regulatory elements of the sequences of Wnt target genes. These molecules act synergistically to retain β-catenin in the nucleus and initiate the activation of Wnt targets. By utilizing Preadipocyte factor-1 (*Pref1*)-*Sox4* transgenic mice, we demonstrated that overexpression of SOX4 diminishes preadipocyte pool while increasing the proportions of MSCs and nonadipogenic lineages, thereby inhibiting the adipocyte hyperplasia. In addition, *Pref1-Sox4* mice were protected from high-fat diet (HFD)-induced obesity. This study hints an association between SOX4 and remodeling of WATs in obesity.

## RESULTS

### SOX4 mediates the antagonistic role BMP4 and TGFβ pathways on preadipocyte determination

Since BMP4 cytokine triggers the development of MSCs toward preadipocytes, while TGFβ exerts an opposite effect, we speculated that the balance of these two pathways is crucial in regulating the preadipocyte determination of MSCs. To test this hypothesis, we first examined the expression profile of TGFβ superfamily regulators and SMAD target genes in BMP4-treated C3H10T1/2 MSCs. Interestingly, *Sox4* showed maximal downregulation (Figure 1A), which was further confirmed by Western blot analysis (Figure 1B). To explore whether SOX4 is involved in BMP4-induced preadipocyte determination, we overexpressed SOX4 in BMP4-treated C3H10T1/2 MSCs and found that the peroxisome proliferator-activated receptor gamma 2 (PPARγ2), a dominant regulator of preadipocyte determination, was markedly inhibited (Figure 1B). To further evaluate the adipogenic potential of these groups, cells were cultured until 2 days post-confluence and induced to differentiation according to the standard adipocyte differentiation procedure (Figure S1A). Oil Red O staining showed remarkably reduced lipid droplets in the SOX4/BMP4-cotreated group compared to the BMP4-treated group (Figure 1C). These results suggested that the overexpression of SOX4 counteracts the effects of BMP4 during the preadipocyte determination of C3H10T1/2 MSCs.

Next, we examined the role of SOX4 on TGFβ signaling-regulated preadipocyte determination. SB431542 is a specific TGFβ receptor kinase inhibitor. Treating the C3H10T1/2 MSCs with SB431542 remarkably

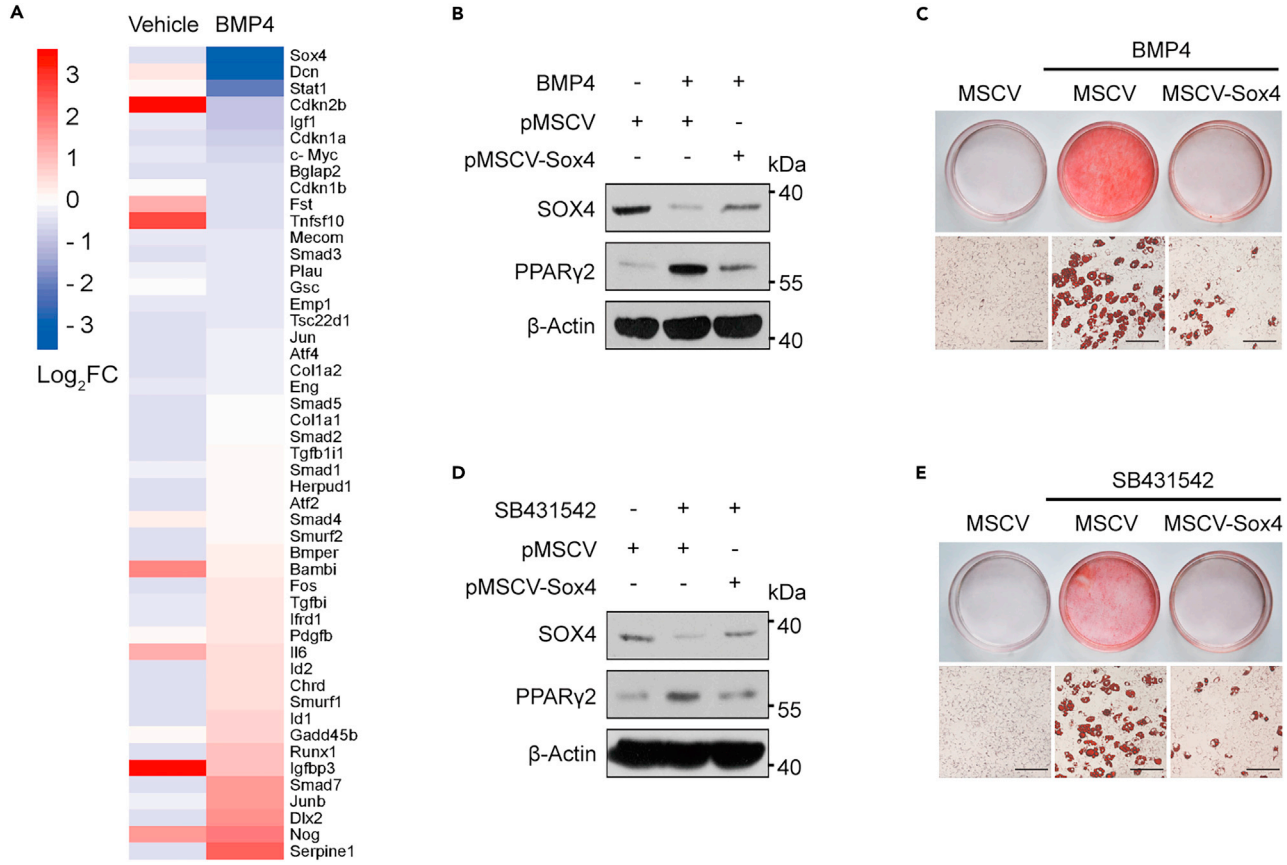


**Figure 1. SOX4 transmits signaling of BMP4 and TGFβ signaling pathways and inhibits preadipocyte determination**

(A) CH10T1/2 cells were cultured with vehicle or 100 ng/mL BMP4 until confluency. TGFβ superfamily regulators and SMAD target genes were examined in these groups and shown in the heatmap. The color scale shows Z scored $log_2$FC representing the mRNA level of each gene in blue (low-expression)-white-red (high-expression) scheme.

(B–E) C3H10T1/2 cells stably expressing *pMSCV* or *pMSCV-Sox4* retrovirus were untreated or treated with 100 ng/mL BMP4 protein (B and C) or 10 μM SB431542 (D and E) until confluency. The levels of *Sox4* and *Pparγ2* proteins in these post-confluent cells were validated by Western blotting (B and D). β-Actin was used as a loading control. To assess the adipogenic differentiation ability, the 2-day post-confluent cells were induced to differentiate for 7 days according to the standard differentiation protocol and analyzed by Oil Red O staining (C and E); scale bar, 200 μm.

downregulated SOX4 expression and increased the PPARγ2 levels (Figures 1D, S1B, and S1C); a similar effect was produced by SMAD2 knockdown (Figures S1D and S1E). On the other hand, SOX4 overexpression strongly inhibited the SB431542-induced PPARγ2 expression during preadipocyte determination (Figure 1D); thus, the adipogenic potential of SOX4/SB431542-cotreated group was greatly impaired (Figure 1E). Consistent with this, treating C3H10T1/2 cells with TGFβ1 to activate the TGFβ signaling pathway, the expression of PPARγ2 was significantly inhibited while the SOX4 level was elevated (Figures S1F and S1G). Knockdown of SOX4 could remove the inhibition role of TGFβ1 on preadipocyte determination, as indicated by increased levels of PPARγ2 and lipogenic genes C/EBPα, FABP4, and adiponectin, as well as the accumulation of lipid droplets (Figures S1F–S1I). These results indicated that SOX4 mediates the inhibitory effect of TGFβ signaling on preadipocyte determination.

Taken together, SOX4 is a mediator for the antagonistic role of BMP4 and TGFβ signaling in the preadipocyte determination program.

## SOX4 inhibition triggers preadipocyte determination and nonadipogenic-adipogenic conversion

To further investigate the role of SOX4 in preadipocyte determination, firstly, we isolated the SVFs of inguinal WATs (iWATs) and performed fluorescence-activated cell sorting analysis using platelet-derived

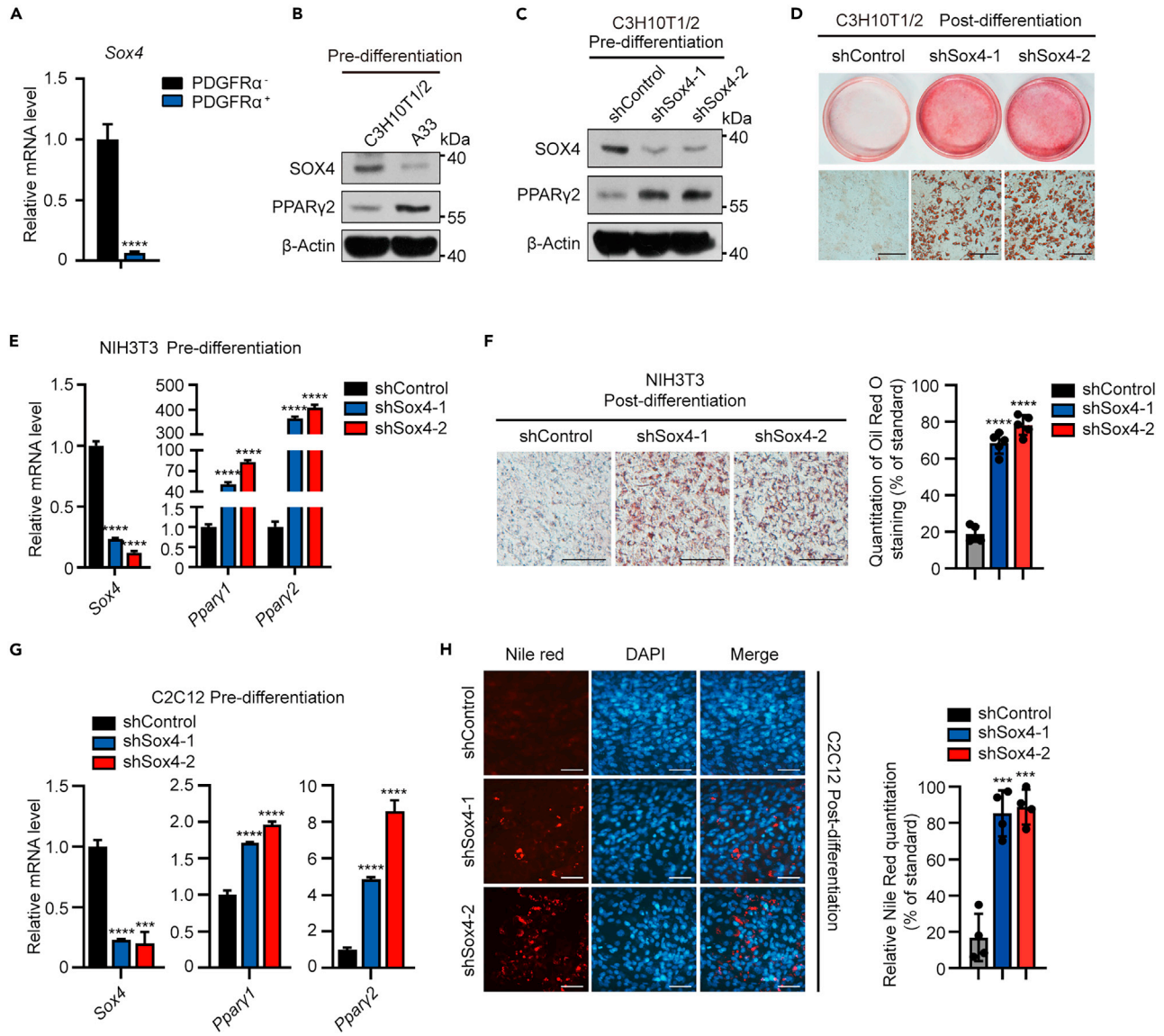


**Figure 2. SOX4 deficiency promotes preadipocyte determination and adipogenic conversion of nonadipogenic lineages**

(A) iWAT SVFs were isolated from adult C57BL/6 mice (8-week-old male mice), and PDGFRα$^-$ and PDGFRα$^+$ cells were sorted by flow cytometry. *Sox4* mRNA levels were determined by qPCR.

(B) The levels of SOX4 and PPARγ2 protein were determined by Western blotting in post-confluent C3H10T1/2 MSCs and A33 preadipocytes.

(C and D) C3H10T1/2 MSCs were stably transfected with *pLKO.1-vector* (shControl) or *pLKO.1-Sox4* (shSox4) and cultured until post-confluence. The levels of SOX4 and PPARγ2 protein were determined by Western blotting (C). 2-day post-confluent cells were induced to differentiate for 7 days and analyzed by Oil Red O staining (D); scale bar, 200 μm.

(E–H) NIH3T3 fibroblasts and C2C12 myoblasts were stably transfected with *pLKO.1-vector* (shControl) or *pLKO.1-Sox4* (shSox4) and cultured until post-confluence. The mRNA levels of *Sox4*, *Pparγ1*, and *Pparγ2* were determined by qPCR (E and G). For NIH3T3 fibroblasts, 2-day post-confluent cells were induced to differentiate for 7 days and analyzed by Oil Red O staining; scale bar, 200 μm (F). For C2C12 myoblasts, the differentiated cells were analyzed by Nile Red staining; scale bar, 100 μm (H). Staining quantifications are obtained from multiple images of a representative experiment.

Data are represented as mean ± SD. ***p < 0.001, ****p < 0.0001.

growth factor receptor α (PDGFRα) antibody (Figure S2A). PDGFRα is a cell surface marker that characterizes the adipocyte precursors, including adipocyte progenitors and preadipocytes. We found that *Sox4* expression in PDGFRα$^+$ adipocyte precursors was much lower than in PDGFRα$^-$ lineages (Figure 2A). Also, SOX4 was highly expressed in C3H10T1/2 MSCs, while PPARγ2 was abundant in committed A33 preadipocytes (Figures 2B and S2B). SOX4 knockdown results in increased PPARγ2 expression in C3H10T1/2

MSCs (Figures 2C and S2C). The MDI (MDI cocktail: isobutylmethylxanthine, dexamethasone, and insulin) treatment induced these SOX4-deficient MSCs to terminal differentiation, as manifested by the upregulation of lipogenic genes, CCAAT enhancer-binding protein α (*C/ebpα*), *Pparγ2*, and *adiponectin*, and the accumulation of lipid droplets in the cells (Figures 2D and S2D). These results demonstrated that inhibition of SOX4 is sufficient to trigger the preadipocyte determination in MSCs.

The conversion between adipocytes and nonadipogenic fibroblasts due to external stimuli or genetic mutations affects the remodeling of adipose tissues and is also associated with obesity-related metabolic dysfunction.[35] To further explore whether the altered SOX4 level mediates the lineage conversion between these two cell types, we knocked down SOX4 by shRNAs in nonadipogenic cell lines (NIH3T3 and C2C12) with strong fibroblastic or myogenic abilities, respectively. The depletion of SOX4 increased the *Pparγ1* and *Pparγ2* levels in a pre-differentiated state in NIH3T3 fibroblasts (Figure 2E). In response to adipocyte differentiation, the expression of lipogenic factors C/EBPα, PPARγ2, and fatty acid-binding protein 4 (Fabp4) increased and the number of lipid-accumulating cells augmented significantly (Figures 2F, S2E, and S2F). In addition, SOX4-deficient C2C12 myoblasts acquired the same gene expression patterns as NIH3T3 fibroblasts in pre- and post-differentiation stages and presented adipocyte-like phenotypes after induction of differentiation (Figures 2G, 2H, S2G, and S2H). These results demonstrated that the inhibition of SOX4 triggers the conversion of nonadipogenic cells into adipogenic lineages.

## Overexpression of SOX4 impairs the adipogenic potential of preadipocytes by modulating the expression of preadipocyte gene profile

Preadipocytes are committed cells with a strong adipogenic capacity, and the expansion of the pool of preadipocytes contributes to the hyperplasia of white adipocytes. In order to determine whether excessive SOX4 impairs the adipogenic capacity of preadipocytes, first, we examined the expression of SOX4 during the differentiation of 3T3-L1 preadipocytes. The results showed a continual and relatively stable expression of SOX4 in 3T3-L1 preadipocytes compared to the dramatically increased lipogenic genes, *Pparγ2* and *Fabp4*, during MDI induction (Figures 3A and 3B). The overexpression of SOX4 strongly inhibited the differentiation of 3T3-L1 preadipocytes, as indicated by the downregulated lipogenic factors and decreased lipid-accumulating cells (Figures 3C–3E). Owing to the low expression of SOX4 in PDGFRα$^+$ precursors and A33 preadipocytes, we speculated that the continuous low expression of SOX4 is required for the cells to maintain preadipocyte status and differentiation potential.

A previous study identified a broad preadipocyte gene expression signature consisting of 53 genes that defined the preadipocyte status: 37 genes abundant in nonadipogenic fibroblasts and 16 genes characteristic of preadipocytes.[36] To explore the molecular mechanisms underlying the adipogenic-nonadipogenic conversion, we analyzed the expression pattern of these preadipocyte signature genes. First, in SOX4-overexpressing 3T3-L1 preadipocytes, 25 genes were significantly upregulated among 37 abundant in nonadipogenic fibroblasts and among the 16 preadipocyte genes, 11 were downregulated (Figure 3F). However, when switching to SOX4-deficient C3H10T1/2 MSCs, of the 37 genes normally abundant in nonadipogenic fibroblasts, 26 were significantly downregulated. Conversely, 14/16 genes were upregulated, indicating the determination of MSCs into preadipocytes (Figure 3F). Zinc finger protein 423 (*Zfp423*) is a key transcriptional regulator of preadipocyte determination.[36] Herein, we compared the altered levels of genes in SOX4-deficient C3H10T1/2 and ZFP423-depleted 3T3-L1 cells and identified 24 overlaps, representing 52.2% of the total 46 modified genes (Figure 3G).

Collectively, these results indicated that overexpression of SOX4 impairs the adipogenic capacity of preadipocytes by altering the preadipocyte gene profile.

## Preadipocyte determination is inhibited by SOX4-LEF1-mediated amplification of Wnt/β-catenin signaling

Several highly evolutionarily conserved signaling pathways, including TGFβ, BMP, Wnt, Notch, and Hedgehog pathways, have been shown to maintain tissue homeostasis by regulating self-renewal as well as early fate determination of MSCs.[13,37–42] Also, previous studies reported that FGFs and PDGFs regulate adipogenesis and chondrogenesis. However, they emerge and function later in the timeline of fate determination process.[43,44] Considering that SOX4 is the downstream target of TGFβ and BMP signaling pathways, and to explore the underlying mechanism of SOX4 in preadipocyte determination, we knocked down SOX4 in C3H10T1/2 MSCs and screened the target genes of Wnt, Notch, and Hedgehog pathways. The results

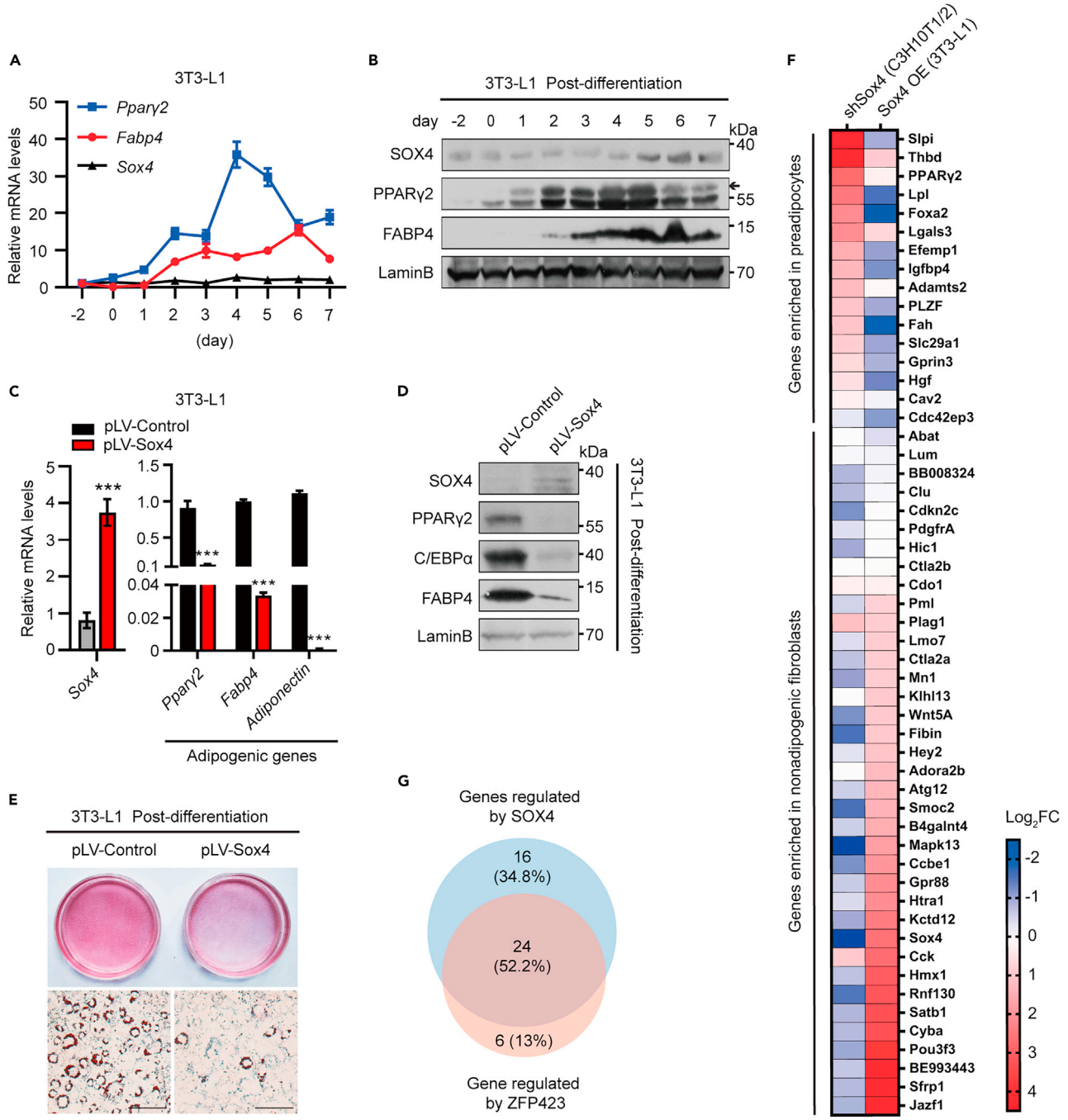


**Figure 3. Overexpression of SOX4 impaired the adipogenic capacity of preadipocytes**

(A and B) 3T3-L1 cells were subjected to adipocyte differentiation and harvested on day −2, 0, 1, 2, 3, 4, 5, 6, and 7 for qRT-PCR and Western blotting analysis of the indicated genes.

(C–E) Control or SOX4-overexpression 3T3-L1 preadipocytes were set up and subjected to differentiation as in method details. On day 7 of differentiation, cells were harvested and subjected to qRT-PCR analysis (C), Western blot (D), and Oil Red O staining assay (E). Scale bar, 200 μm.

(F) Expression of genes included in the preadipocyte gene profile in SOX4-deficient C3H10T1/2 MSCs and SOX4-overexpressing 3T3-L1 preadipocytes. The different colors represent the fold-changes relative to the corresponding control group. The control group corresponding to the SOX4 KD group was C3H10T1/2 cells infected with *pLKO.1-Vector* lentivirus, and the control group corresponding to the SOX4 OE group was 3T3-L1 cells infected with *pLV-EF1A-Null* lentivirus.

(G) Overlap between SOX4-dependent genes (<0.8-fold change or >2-fold change in SOX4-deficient C3H10T1/2 MSCs) and ZFP423-dependent genes among the preadipocyte gene profile.

Data are represented as mean ± SD. ***p < 0.001.

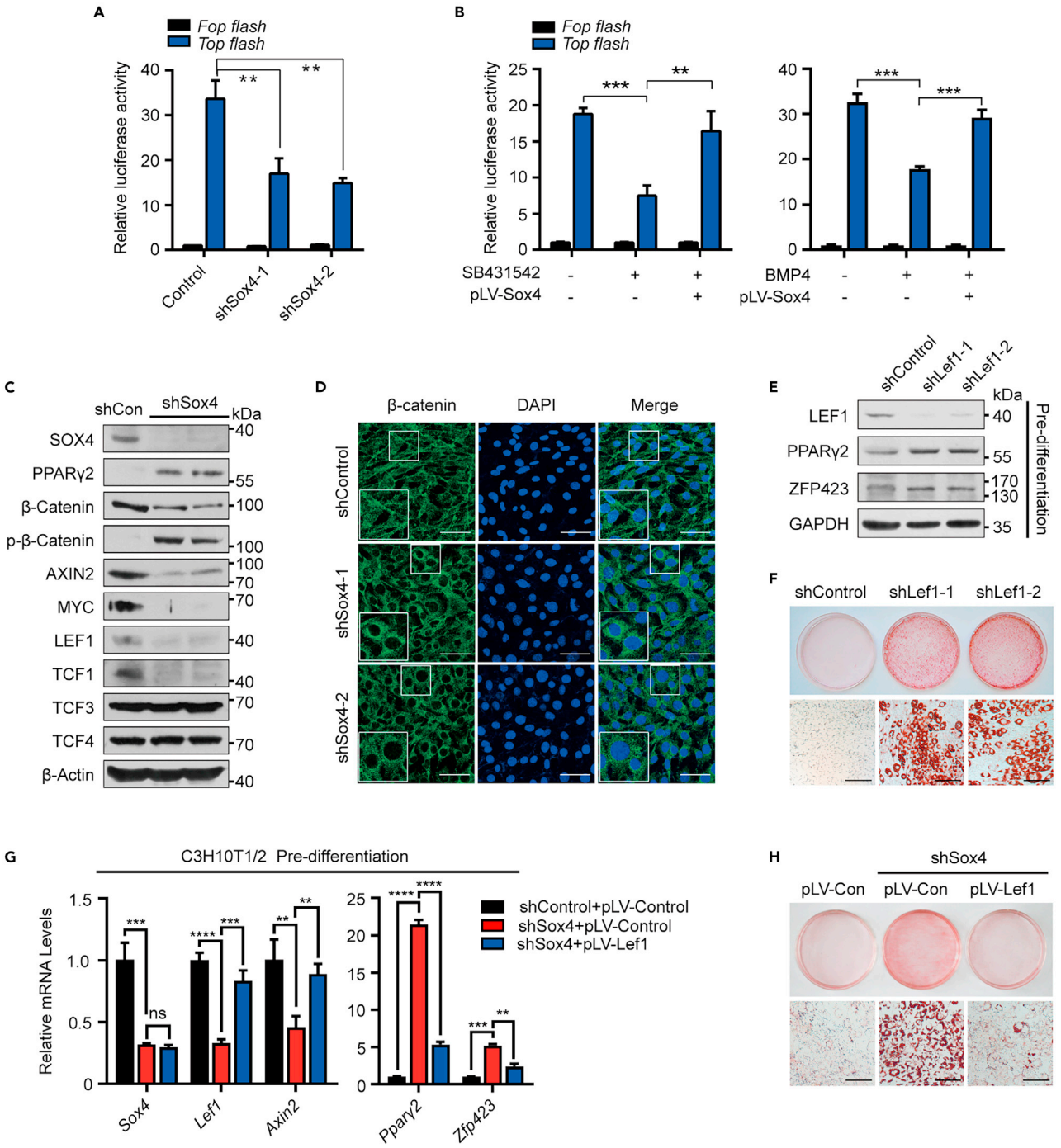


**Figure 4. SOX4 inhibits preadipocyte determination by activating LEF1 expression**

(A) C3H10T1/2 MSCs stably expressing *pLKO.1-Control* (Control) or *pLKO.1-Sox4* were transiently transfected with *SuperTOP/FOP* flash and *β-gal* plasmids. The activities of Wnt signaling pathway were measured using luciferase assay. *SuperFOPflash* consists of Wnt-responsive elements that are mutants and used as a negative control.

(B) SOX4-overexpressing C3H10T1/2 MSCs were exposed to 10 μM SB431542 (left) or 100 ng/mL BMP4 (right) and the corresponding vehicle. The activities of Wnt signaling pathway in these cells were measured by luciferase assay.

(C) Protein levels of SOX4 and Wnt components were analyzed by Western blotting in pre-differentiated control and SOX4-deficient C3H10T1/2 MSCs.

(D) Immunofluorescence staining of β-catenin (green) and DAPI (blue) in control and SOX4-deficient C3H10T1/2 MSCs. Scale bar, 50 μm.

(E) Protein levels of LEF1, PPARγ2, and ZFP423 were analyzed by Western blotting in the control and LEF1-deficient C3H10T1/2 MSCs. GAPDH was used as a loading control.

**Figure 4. *Continued***

(F) 2-day post-confluent control and LEF1-deficient C3H10T1/2 MSCs were induced to differentiate for 7 days and analyzed by Oil Red O staining. Scale bar, 200 μm.

(G and H) Relative mRNA levels (G) of indicated genes were analyzed by qPCR in pre-differentiated control or SOX4-deficient C3H10T1/2 MSCs virally expressing *pLV-Control* and *pLV-Lef1*. 2-day post-confluent cells were induced to differentiate for 7 days and analyzed by Oil Red O staining (H). Scale bar, 200 μm.

Data are represented as mean ± SD. ns, no significance, **p < 0.01, ***p < 0.001, ****p < 0.0001.

showed that Wnt target genes were downregulated, while those in the Notch and Hedgehog signaling pathways showed no or only a partial response (Figure S3A). Consistently, LEF/TCF-dependent *TOPFlash* luciferase assay revealed a significant decrease in Wnt signaling activity in SOX4-deficient MSCs (Figure 4A). Moreover, the treatment of C3H10T1/2 MSCs with SB431542 or BMP4 significantly downregulated the activities of the Wnt signaling pathway, which were largely recovered after the overexpression of SOX4 (Figure 4B). These findings implied that SOX4 is an intermediary component linking the TGFβ and BMP4 signaling pathways with the Wnt signaling pathway.

To further explore the SOX4-modulated Wnt signaling pathway in the program of preadipocyte determination, we examined the key components of canonical Wnt signaling pathway in SOX4-deficient C3H10T1/2 MSCs. The dramatic downregulation of Wnt targets AXIN2 and MYC, further confirming that the Wnt signaling pathway was regulated in a SOX4-dependent manner (Figures 4C and S3A). β-Catenin is a nucleocytoplasmic shuttle protein. Its localization and stability depend on the interaction with GSK-3β/APC/AXIN or TCF/LEF through a competition mechanism.[45–49] Herein, we observed that both the total content and the nuclear localization of the β-catenin protein were decreased markedly (Figures 4C and 4D), while the level of phosphorylated β-catenin was increased in SOX4-deficient C3H10T1/2 MSCs (Figure 4C). Moreover, LEF1 and TCF1, two major transcription factors interacted with β-catenin and initiated the transcription of Wnt target genes in the nucleus, declined sharply after SOX4 depletion (Figures 4C and S3A), while the other Wnt transcriptional factors, TCF3 and TCF4, remained unchanged (Figures 4C and S3A). To further examine the roles of TCF/LEF transcription factors in the preadipocyte determination program, TCF1, TCF3, TCF4, and LEF1 were knocked down in C3H10T1/2 cells, respectively (Figures 4E and S4A–S4C). However, only LEF1 knockdown increased the expression of the preadipocyte determinant factors, PPARγ2 and ZFP423 (Figures 4E and S4A–S4C). Subsequently, these cells successfully differentiated into mature adipocytes when subjected to a standard adipocyte differentiation program compared to the control group (Figures 4F and S4D–S4J). Also, *Lef1* showed a lower expression after BMP4 and SB431542 treatment (Figure S4K). On the other hand, the overexpression of LEF1 compensated for the effects caused by SOX4 loss at the genetic and phenotype levels (Figures 4G, 4H, and S4L). These data suggest that the inhibition of SOX4 on preadipocyte determination is dependent on LEF1.

As described previously, SOX4 deficiency reduces the nuclear colocalization of β-catenin, the vital coactivator in the Wnt transcriptional complex. Next, we investigated whether SOX4 exerts an architectural role in the assembly of Wnt transcriptional complex. Endogenous immunoprecipitation assays using β-catenin, SOX4, and LEF1 antibodies showed interactions between SOX4 and β-catenin as well as LEF1 (Figures 5A–5C). Further *in vitro* pull-down assays demonstrated that SOX4 directly binds to β-catenin and LEF1 (Figures S5A and S5B). The confocal images showed a clear colocalization of the three proteins (Figure 5D). The knockdown of SOX4 significantly attenuated the binding between β-catenin and LEF1 protein, which confirmed the critical role of Sox4 in maintaining the stability of the Wnt transcriptional complex (Figure 5E). Next, we assessed whether the β-catenin/SOX4/LEF1 complex directly activates the transcription of *Lef1* and Wnt targets. As shown in Figure 5F, the gene sequences of *Lef1*, *Axin2*, and *Ccnd1* containing the adjacent LEF1- and SOX4-binding sites, predicted by JASPAR, were cloned into a PGL4.26 promoter-less luciferase reporter cassette. In transfection with *pLV-N-Flag-SOX4* or cotransfection with *pLV-HA-β-catenin* and *pLV-Lef1*, these fragments were sufficient to initiate varying degrees of the luciferase reporter activity in C3H10T1/2 MSCs (Figure 5F). Significantly enhanced activities of these reporters were conferred by a cotransfection with *pLV-N-Flag-SOX4*, *pLV-HA-β-catenin*, and *pLV-Lef1* (Figure 5F). Interestingly, deletion of SOX4-binding sites adjacent to the LEF1-binding sites compromised the luciferase activity, despite co-overexpression of β-catenin, LEF1, and SOX4 (Figure 5F). In a chromatin immunoprecipitation assay, SOX4 occupied the +261 site downstream of the *Lef1* transcription start site in a LEF1-dependent manner (Figure 5G). These results indicated that SOX4 functions as an essential transcription factor in the transcriptional activation of *Lef1* and Wnt targets.

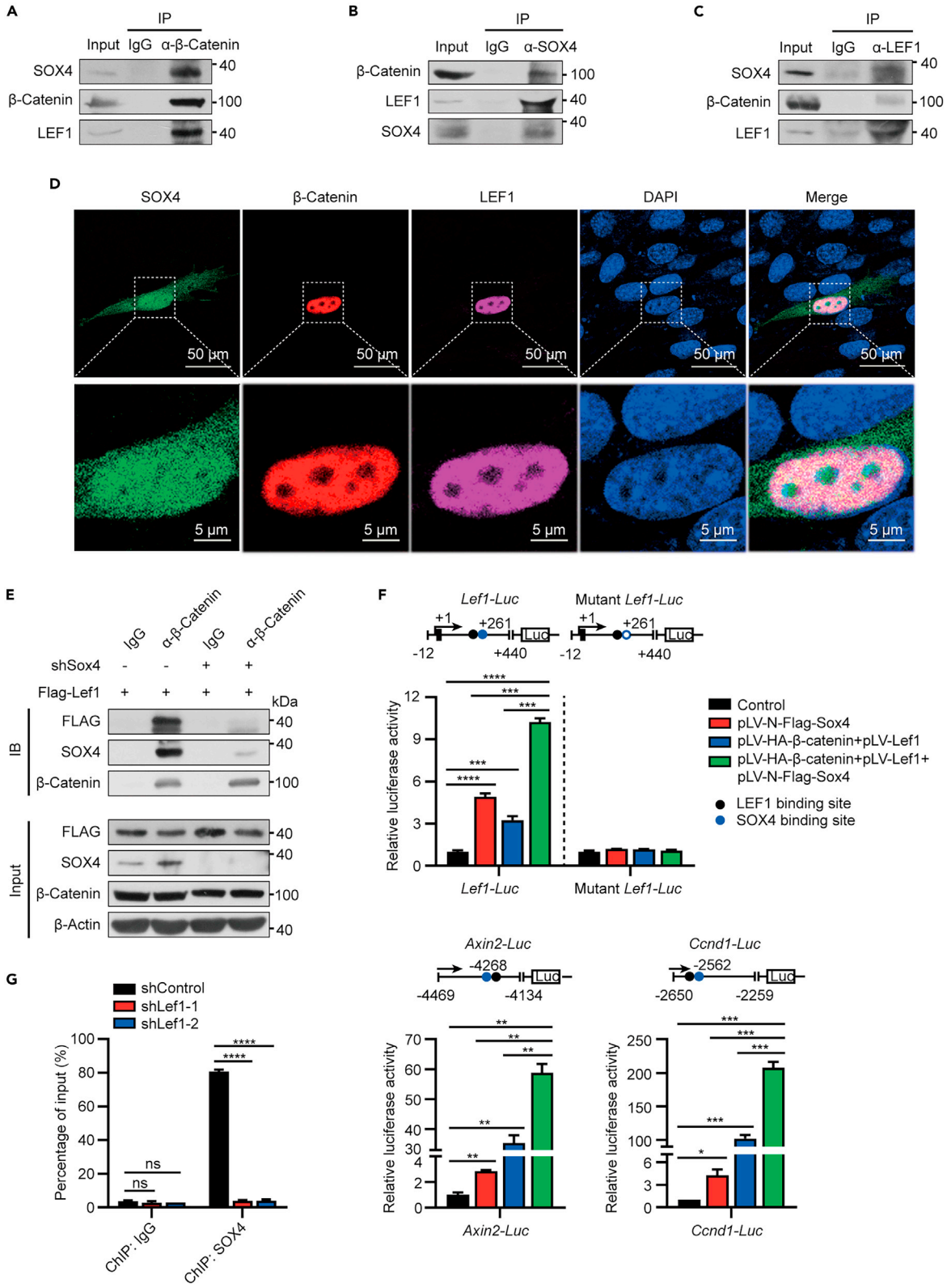
A
IP
Input IgG α-β-Catenin
SOX4
β-Catenin
LEF1
40
100
40
B
IP
Input IgG α-SOX4
β-Catenin
LEF1
SOX4
100
40
40
C
IP
Input IgG α-LEF1
SOX4
β-Catenin
LEF1
40
100
40
D
SOX4
β-Catenin
LEF1
DAPI
Merge
50 μm
5 μm
E
IgG
α-β-Catenin
IgG
α-β-Catenin
shSox4 - - + +
Flag-Lef1 + + + +
kDa
IB
FLAG
SOX4
β-Catenin
40
40
100
Input
FLAG
SOX4
β-Catenin
β-Actin
40
40
100
40
F
Lef1-Luc
Mutant Lef1-Luc
+1
+261
Luc
-12
+440
Relative luciferase activity
Control
pLV-N-Flag-Sox4
pLV-HA-β-catenin+pLV-Lef1
pLV-HA-β-catenin+pLV-Lef1+
pLV-N-Flag-Sox4
LEF1 binding site
SOX4 binding site
Axin2-Luc
-4268
-4469
-4134
Ccnd1-Luc
-2562
-2650
-2259
G
shControl
shLef1-1
shLef1-2
Percentage of input (%)
ns
ChIP: IgG
ChIP: SOX4

**Figure 5. SOX4 enhances the transcription of Wnt targets by forming a complex with β-catenin and LEF1**

(A–C) C3H10T1/2 cell lysates were prepared and immunoprecipitated with β-catenin (A), SOX4 (B), and LEF1 (C) antibodies, respectively. The endogenous combination between β-catenin, SOX4, and LEF1 was analyzed by Western blotting.

(D) C3H10T1/2 cells were co-transfected with *pLV-EF1A-Sox4*, *mCherry-β-catenin*, and *pLV-flag-Lef1*. The colocalization of SOX4, β-catenin, and LEF1 protein was confirmed by high-resolution imaging, Scale bar, 50 μm. Boxed areas are shown at higher magnification in the insets, Scale bar, 5 μm.

(E) Control and SOX4-knockdown C3H10T1/2 MSCs were stably transfected with *pLV-flag-Lef1*, and immunoprecipitation was performed with IgG and β-catenin antibodies in these cells. Samples were assessed by Western blotting.

(F) Luciferase reporters consisting of adjacent SOX4 and LEF1 binding elements or only missing SOX4 binding elements were constructed (as shown in the schematic) and co-transfected with indicated plasmids as well as *β-gal* into the C3H10T1/2 cells. The transcriptional activities of the indicated genes were analyzed by luciferase assay.

(G) The binding of SOX4 protein on the site +261 downstream of the *Lef1* TSS was assessed by ChIP using SOX4 antibody in the control and LEF1-deficient C3H10T1/2 MSCs. The immunoprecipitates were purified and analyzed by qPCR.

Data are represented as mean ± SD. ns, no significance, *p < 0.05, **p < 0.01, ***p < 0.001, ****p < 0.0001.

Since both SOX4 and LEF1 bind to the adjacent sites on promoters of target genes, and LEF1 is indispensable for SOX4 function, we analyzed the conserved binding elements of SOX4 and LEF1 on promoters of the 27 nonadiopgenic fibroblast genes which were included in preadipocyte gene expression signature and positively regulated by SOX4 using JASPAR. The result showed that 26 of the 27 genes (approximately 96.3%) have this LEF1/SOX4 double-binding sites on their promoters (Figure S5C). Given that SOX4 also enhances the association between β-catenin and LEF1, we speculate that SOX4 and LEF1 provide a platform for the assembly of canonical Wnt transcriptional activation complex.

Together, these results established that SOX4 cooperates with LEF1 to facilitate the β-catenin nuclear retention, thereby activating the Wnt signaling pathway and inhibiting preadipocyte determination.

## Overexpression of SOX4 *in vivo* diminishes the pool of preadipocytes

*In vitro* studies have demonstrated that SOX4 inhibits preadipocyte determination and triggers a conversion to nonadipogenic lineage. Herein, we aimed to determine whether SOX4 overexpression inhibits the generation of primary preadipocytes *in vivo*. *Pref1* gene is highly expressed in preadipocytes but disappears during differentiation and is defined as a marker of preadipocytes derived from the mesenchyme.[50–53] Besides, Pref1 has shown better spatiotemporal specificity than PDGFRα with respect to preadipocyte determination.[8,54,55] Hence, we generated a mouse model that expresses SOX4 under the control of a 6-kbp *Pref1* promoter fragment (*Pref1-Sox4*) (Figure 6A). Previous study has shown that prolonged high-fat feeding (2 months of HFD exposure) induces a low rate of hyperplasia in subcutaneous adipose tissues.[56] Our previous study also found that exposing 3-week-old WT mice and *Pref1-Sox4* mice to an HFD condition for 4 months significantly widened the differences in body weight and induced metabolic disorders.[57] Herein, we treated 3-week-old WT mice and *Pref1-Sox4* mice with normal chow diet (NCD) or HFD for 20 weeks to maximize the differences. iWAT SVFs from NCD- or HFD-fed wild-type (WT) and *Pref1-Sox4* groups were isolated and analyzed by qPCR and Western blot (Figures 6B and 6C). We found that SOX4 overexpression efficiency was much higher in HFD group than that in NCD group, possibly due to enhanced transcriptional activation of *Pref1* in HFD (Figures 6B, 6C, and S6A). Since iWAT SVFs are composed of multiple cell types, including vascular cells, mesenchymal progenitors, adipose precursors, and fibroblast-like cells,[58] we further investigated which subtype of cells overexpress SOX4 using flow cytometry and qPCR. PDGFRα is widely accepted as a cell surface marker of adipose precursors in adipose tissues.[52,54,59] Merrick et al. identified DPP4-expressing ($DPP4^+$) cells as highly proliferative multipotent mesenchymal progenitors and ICAM1-expressing ($ICAM1^+$) cells as committed preadipocytes.[8] By examining mRNA levels of *Sox4* in these subpopulations, we found that the SOX4 overexpression driven by the *Pref1* promoter was mainly in preadipocytes, rather than in mesenchymal progenitors (Figure 6D).

The preceding data imply that SOX4 may inhibit the generation of preadipocytes *in vivo*. To test this hypothesis, we administered NCD or HFD to WT and *Pref1-Sox4* mice for 20 weeks and analyzed the cell populations with adipogenic potential by flow cytometry. First, the SVFs were isolated and fractioned by Lin markers (CD31, CD45, and Ter119) to sort out the nonadipogenic lineages and by PDGFRα for adipocyte precursors, including adipocyte progenitors and preadipocytes (Figure S6B).[60] The percentages of $Lin^-$: $PDGFR\alpha^+$ adipocyte precursors did not change in WT and *Pref1-Sox4* mice fed with NCD (Figure 6E). However, when switched to long-term HFD, the proportion of this population significantly increased in WT mice, but this effect was apparently suppressed by overexpression of SOX4 (Figure 6E). To further explore whether SOX4 overexpression alters the proportion of mesenchymal progenitors and preadipocytes, we

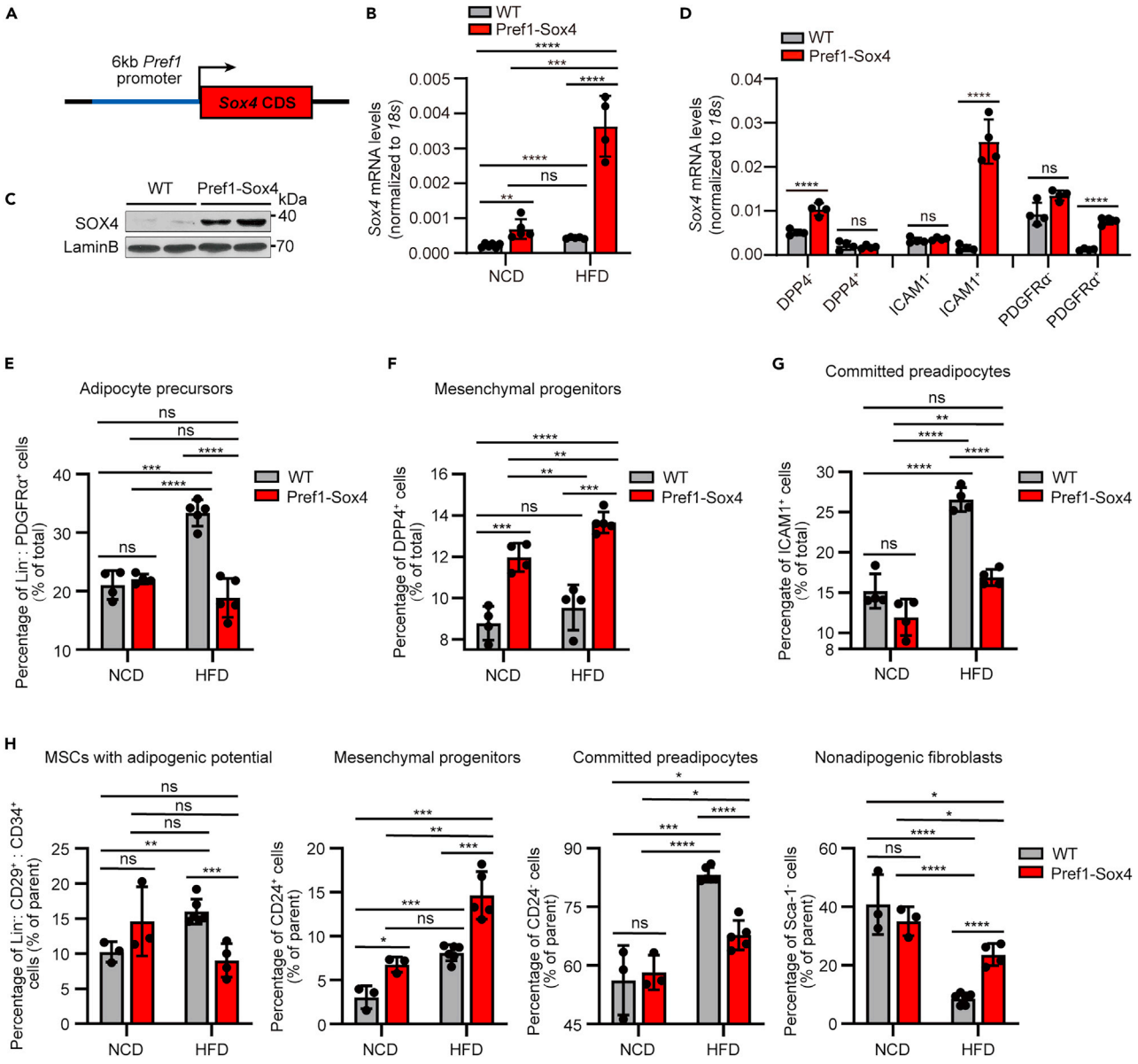


**Figure 6. Overexpression of SOX4 in preadipocytes diminished the pool of preadipocytes under HFD condition**

3-week-old WT and *Pref1-Sox4* mice were housed at room temperature and fed with NCD or HFD for 20 weeks.

(A) *Pref1-Sox4* mice were generated by directly inserting coding sequence (CDS) sequence of *Sox4* after a 6-kbp fragment upstream of the transcriptional start site of the *Pref1* promoter.

(B) iWAT SVFs were isolated from NCD or HFD-fed WT and *Pref1-Sox4* mice and cultured for 2 h to exclude the non-adherent cells. Then, the cultured cells were collected and the expression of *Sox4* was detected by qPCR (n = 4–6). mRNA levels were normalized to 18s RNA. The mean CT was converted to relative expression value by the equation $2^{-\Delta Ct}$.

(C) The expression of SOX4 in iWAT SVFs of HFD-fed WT and *Pref1-Sox4* mice was detected by Western blotting.

(D) The expression of *Sox4* in indicated cell populations sorted by flow cytometry was examined by qPCR (n = 4). mRNA levels were normalized to 18s RNA. The mean CT was converted to relative expression value by the equation $2^{-\Delta Ct}$.

(E–G) The proportions of $CD45^-$: $CD31^-$: $Ter119^-$: $PDGFR\alpha^+$ ($Lin^-$: $PDGFR\alpha^+$ cells) adipocyte precursors (E), $DPP4^+$ MSCs (F) and $ICAM1^+$ preadipocytes (G) were analyzed by flow cytometry in NCD- and HFD-fed WT and *Pref1-Sox4* mice (NCD group: n = 4; HFD: n = 4–5).

(H) The proportions of MSCs with adipogenic potential ($Lin^-$: $CD34^+$: $CD29^+$), adipocyte progenitors ($Lin^-$: $CD34^+$: $CD29^+$: $Sca\text{-}1^+$: $CD24^+$, $CD24^+$ cells), committed preadipocytes ($Lin^-$: $CD34^+$: $CD29^+$: $Sca\text{-}1^+$: $CD24^-$, $CD24^-$ cells), and nonadipogenic fibroblasts ($Lin^-$: $CD34^+$: $CD29^+$: $Sca\text{-}1^-$, $Sca\text{-}1^-$ cells) were analyzed by flow cytometry in NCD- and HFD-fed WT and *Pref1-Sox4* mice (NCD group: n = 3; HFD: n = 4–6).

3-week-old WT and *Pref1-Sox4* mice with HFD for 20 weeks were used in this study.

Data are represented as mean ± SD. ns, no significance, *p < 0.05, **p < 0.01, ***p < 0.001, ****p < 0.0001.

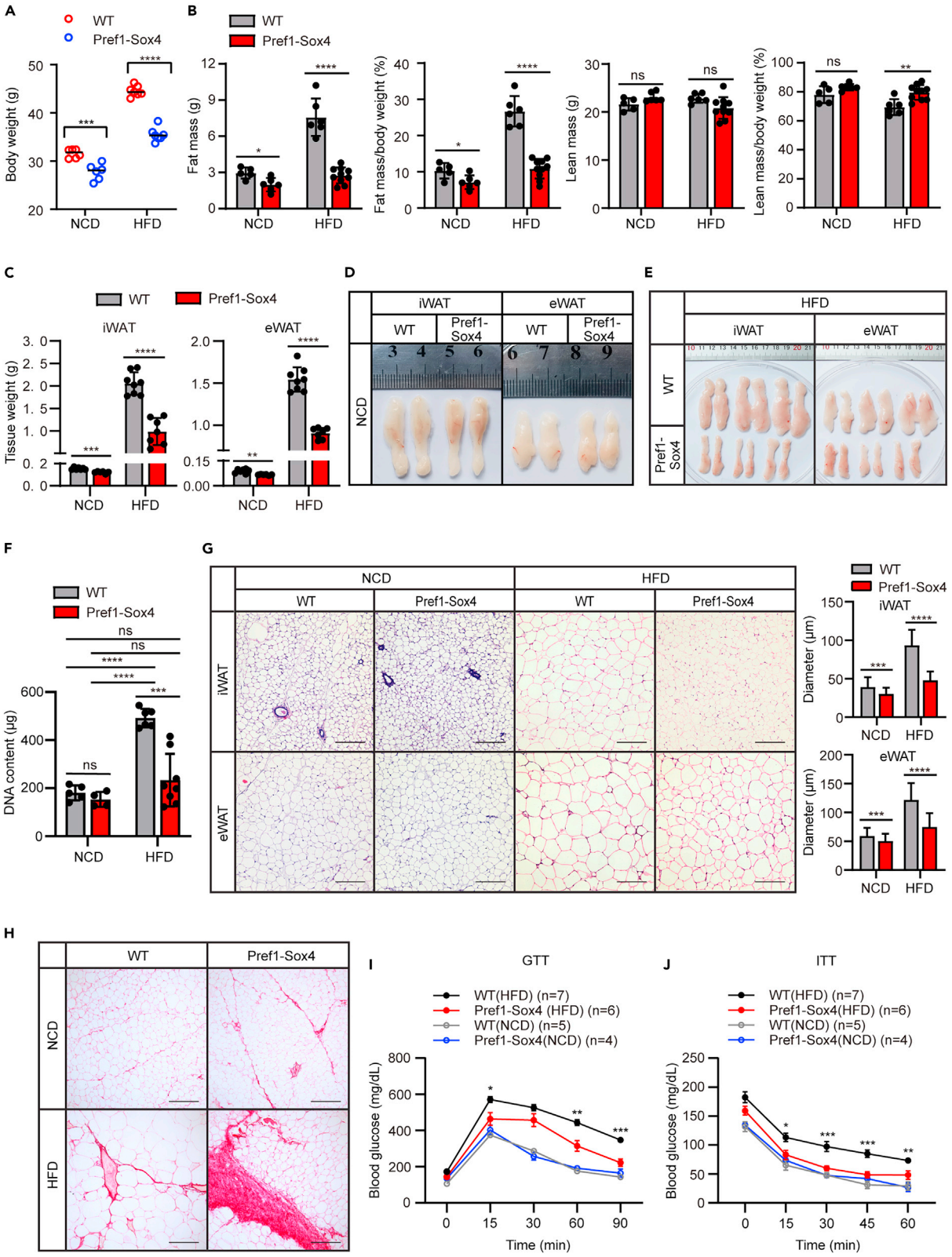
A
WT
Pref1-Sox4
Body weight (g)
NCD
HFD
B
Fat mass (g)
Fat mass/body weight (%)
Lean mass (g)
Lean mass/body weight (%)
ns
C
iWAT
eWAT
Tissue weight (g)
D
E
HFD
F
DNA content (μg)
G
Diameter (μm)
H
I
GTT
WT(HFD) (n=7)
Pref1-Sox4 (HFD) (n=6)
WT(NCD) (n=5)
Pref1-Sox4(NCD) (n=4)
Blood glucose (mg/dL)
Time (min)
J
ITT
Pref1-Sox4(HFD) (n=6)
Pref1-Sox4(NCD) (n=4)

**Figure 7. SOX4 protects mice from HFD-induced obesity and promotes fibrogenesis *in vivo***

3-week-old WT and *Pref1-Sox4* mice were housed at room temperature and fed with NCD or HFD for 20 weeks.

(A) Body weight of WT and *Pref1-Sox4* mice fed with NCD (n = 6) or HFD for 14 weeks (n = 7).

(B) Body composition of WT and *Pref1-Sox4* mice fed with NCD (n = 5–6) or HFD for 10 weeks (n = 6–10).

(C) Tissue weight of iWAT and eWAT in WT and *Pref1-Sox4* mice fed with NCD (n = 6–7) or HFD (n = 7–8) for 20 weeks.

(D and E) Representative images of iWATs and eWATs WT and *Pref1-Sox4* mice fed with NCD (B) or HFD (C) for 20 weeks.

(F) Total DNA content of mature adipocytes in iWAT isolated from WT and *Pref1-Sox4* mice fed NCD (n = 4–5) or HFD (n = 6–8) for 20 weeks.

(G) Representative H&E staining images of iWATs and eWATs from WT and *Pref1-Sox4* mice fed with NCD or HFD for 20 weeks. Scale bar, 200 μm. The histograms on the right represent the average diameters of adipocytes in each group.

(H) Representative Sirius Red staining of iWAT from WT and *Pref1-Sox4* mice fed NCD or HFD for 20 weeks. Scale bar, 200 μm.

(I and J) GTT (I) and ITT (J) were performed in WT and *Pref1-Sox4* mice fed with NCD or HFD for 20 weeks.

Data are represented as mean ± SD. ns, no significance, *p < 0.05, **p < 0.01, ***p < 0.001, ****p < 0.0001.

performed flow cytometry using DPP4 and ICAM1 antibodies (Figures S6C and S6D). We found that prolonged HFD did not alter the proportions of $DPP4^+$ MSCs, but overexpression of SOX4 significantly increased the proportions of $DPP4^+$ MSCs in HFD groups (Figure 6F). Unlike $DPP4^+$ MSCs, the generation of $ICAM1^+$ preadipocytes was highly induced by HFD and largely suppressed by SOX4 to the same level as in the NCD-fed WT mice (Figure 6G). Then, the adipogenic cell populations were fractionated based on the combination of different cell surface markers to isolate adipocyte progenitors, committed preadipocytes, and nonadipogenic fibroblasts.[58,61–63] As shown in Figure 6H, the proportions of $Lin^-$: $CD34^+$: $CD29^+$ stem cell population with adipogenic potential increased significantly with the transition from NCD to HFD, but decreased in HFD-fed *Pref1-Sox4* mice to the same levels as in the NCD-fed WT group (Figures 6H and S6E). Next, the $Lin^-$: $CD34^+$: $CD29^+$ subpopulations were further separated based on additional staining for Sca-1 and CD24 to enable isolation of adipocyte progenitors capable of considerable expansion and preadipocytes with highly adipogenic capacity (Figure S6E). The results showed that both the proportions of $Lin^-$: $CD34^+$: $CD29^+$: $Sca\text{-}1^+$: $CD24^+$ ($CD24^+$) adipocyte progenitors and the proportions of $Lin^-$: $CD34^+$: $CD29^+$: $Sca\text{-}1^+$: $CD24^-$ ($CD24^-$) preadipocytes were significantly increased upon diet switch (Figure 6H). Overexpression of SOX4 reduced the proportion of $CD24^-$ preadipocytes but increased the proportion of $CD24^+$ adipocyte progenitors and $Lin^-$: $CD34^+$: $CD29^+$: $Sca\text{-}1^-$ ($Sca1^-$) low-adipogenic fibroblasts, implying inhibited preadipocyte generation and enhanced potential for conversion to low-adipogenic fibroblasts and earlier adipocyte progenitors in *Pref1-Sox4* mice fed with HFD (Figure 6H).

Collectively, these data indicated that overexpression of SOX4 altered the cellular composition of WAT through reducing the pool of preadipocytes and increasing the lineages with nonadipogenic potential.

## *Pref1-Sox4* mice were protected from HFD-induced adiposity

Given that preadipocytes residing in fat depots undergo mitotic proliferation and adipogenic differentiation, thereby accelerating the expansion of adipose tissues *in vivo*,[3] we speculated that SOX4 overexpression could suppress the enlargement of WAT depot. To test this hypothesis, 3-week-old WT and *Pref1-Sox4* mice were fed an NCD or an HFD for 20 weeks and the body weight and composition were examined subsequently. The results showed that the body weight and fat percentage of *Pref1-Sox4* mice were significantly lower than those of WT mice under HFD condition, while that of the NCD-fed group only decreased slightly, with no significant change in lean mass and percentage (Figures 7A and 7B). Consistent with this, the weight and size of iWATs and epididymal WATs (eWATs) of *Pref1-Sox4* mice in the HFD group were significantly reduced, while those in the NCD group were slightly decreased, indicating a slower rate of fat growth in *Pref1-Sox4* mice (Figures 7C–7E). To explore whether the hyperplasia of white adipocytes is impaired due to a diminishment in the preadipocyte pool, we collected mature adipocytes from iWAT of WT and *Pref1-Sox4* mice fed with NCD or HFD. Total DNA quantification revealed a remarkable increase in DNA content in HFD-fed WT mice, suggesting a prominent adipocyte hyperplasia occurred in diet switch (Figure 7F). However, this hyperplasia was largely attenuated by SOX4 overexpression, as manifested by significantly reduced DNA content in HFD-fed *Pref1-Sox4* mice (Figure 7F). Moreover, histologic section and H&E staining of iWAT and eWAT showed that the white adipocytes of *Pref1-Sox4* mice fed with HFD were much smaller than those of WT mice (Figure 7G). Also, Sirius Red staining revealed more obvious fibrogenesis in iWAT of *Pref1-Sox4* mice (Figure 7H). On the other hand, the difference between NCD-fed WT and *Pref1-Sox4* mice was less significant (Figures 7G and 7H). Further experiment found that overexpression of SOX4 alleviated glucose intolerance as well as insulin resistance in HFD-fed *Pref1-Sox4* mice (Figures 7I and 7J), which was also confirmed by another research published previously by our research group.[57] In conclusion, these results highlighted the critical role of SOX4 in combating HFD-induced adiposity and maintaining glucose homeostasis.

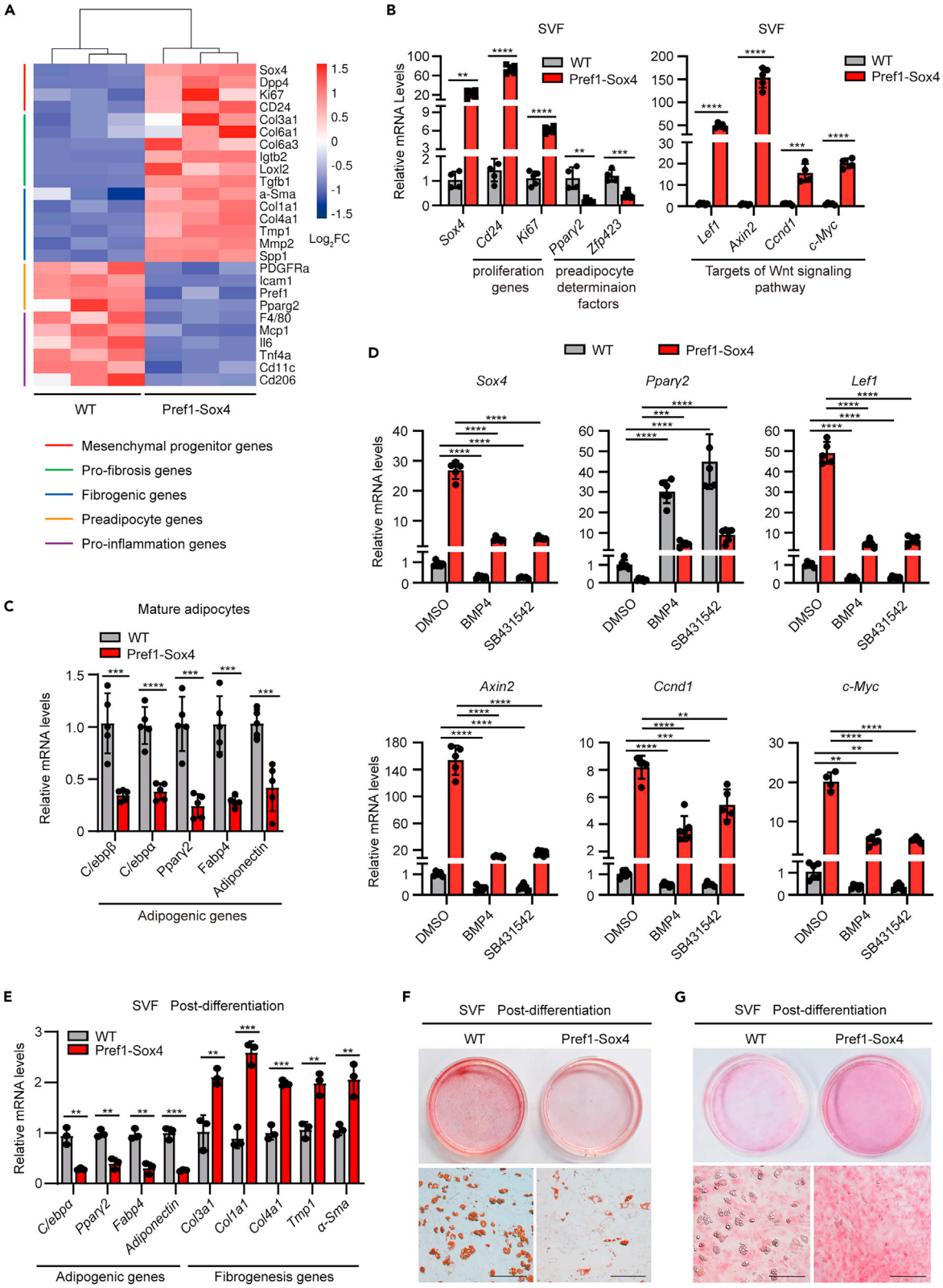
A
Sox4
Dpp4
Ki67
CD24
Col3a1
Col6a1
Col6a3
Igtb2
Loxl2
Tgfb1
a-Sma
Col1a1
Col4a1
Tmp1
Mmp2
Spp1
PDGFRa
Icam1
Pref1
Pparg2
F4/80
Mcp1
Il6
Tnf4a
Cd11c
Cd206
1.5
1
0.5
0
-0.5
-1
-1.5
Log2FC
WT
Pref1-Sox4
Mesenchymal progenitor genes
Pro-fibrosis genes
Fibrogenic genes
Preadipocyte genes
Pro-inflammation genes
B
SVF
WT
Pref1-Sox4
Relative mRNA Levels
Sox4
Cd24
Ki67
Pparγ2
Zfp423
proliferation genes
preadipocyte determinaion factors
Lef1
Axin2
Ccnd1
c-Myc
Targets of Wnt signaling pathway
C
Mature adipocytes
Relative mRNA levels
C/ebpβ
C/ebpα
Pparγ2
Fabp4
Adiponectin
Adipogenic genes
D
Sox4
Pparγ2
Lef1
Axin2
Ccnd1
c-Myc
DMSO
BMP4
SB431542
E
SVF Post-differentiation
Col3a1
Col1a1
Col4a1
Tmp1
α-Sma
Adipogenic genes
Fibrogenesis genes
F
SVF Post-differentiation
G
SVF Post-differentiation

**Figure 8. SOX4 mediates crosstalk between the BMP4 and TGFβ signaling pathways and activates the Wnt signaling pathway *in vivo***

(A) iWATs were isolated from WT and *Pref1-Sox4* mice fed HFD for 20 weeks, and the mesenchymal progenitor, pro-fibrosis, fibrogenic, preadipocyte, and pro-inflammation genes were examined and shown in the heatmap. The color scale shows Z scored $log_2$FC representing the mRNA level of each gene in blue (low expression)-white-red (high expression) scheme.

(B) mRNA levels of indicated genes were analyzed by qPCR in iWAT SVFs of WT and *Pref1-Sox4* mice fed HFD for 20 weeks (n = 4–5).

(C) mRNA levels of lipogenic genes were analyzed by qPCR in mature white adipocytes from iWAT of WT and *Pref1-Sox4* mice fed HFD for 20 weeks (n = 5).

(D) PDGFRα$^+$ cells were sorted from iWATs of WT and *Pref1-Sox4* mice by FACS and then treated with 100 ng/mL BMP4 or 10 μM SB431542 as method described before harvest. The relative mRNA levels of indicated genes were assessed by qPCR (n = 4–6).

(E–G) 3-week-old WT mice and *Pref1-Sox4* mice were fed with HFD for 20 weeks. SVFs were isolated and subjected to adipocyte differentiation. The mRNA levels of lipogenic genes and fibrogenesis genes were analyzed by qPCR (E). The lipid accumulation and fibrogenesis were analyzed by Oil Red O staining (F) and Sirius Red staining (G), respectively. Scale bar, 200 μm.

Data are represented as mean ± SD. **p < 0.01, ***p < 0.001, ****p < 0.0001.

## BMP4/TGFβ-SOX4-Wnt cascade regulates the preadipocyte determination and WAT gene expression profiles *in vivo*

Since HFD-fed *Pref1-Sox4* mice had much higher SOX4 overexpression efficiency and showed obvious phenotypic changes compared to corresponding WT group, we asked whether the changes in gene expression signature were associated with preadipocyte determination. 3-week-old WT mice and *Pref1-Sox4* mice were fed with HFD for 20 weeks and the total mRNA of iWATs was extracted and analyzed by qPCR. The results demonstrated that of the 26 significantly altered genes, 15 were significantly upregulated mesenchymal stem cell genes, pro-fibrosis genes, and fibrogenic genes, and 11 were preadipocyte and pro-inflammation genes inhibited by SOX4 (Figure 8A). To explore whether the molecular mechanisms by which SOX4 functions could be recapitulated in HFD-induced obesity, we isolated iWAT SVFs and mature adipocytes from WT and *Pref1-Sox4* mice fed with HFD for 20 weeks and examined the expression of proliferation genes, preadipocyte determination factors, Wnt signaling molecules, and adipogenesis genes. Both preadipocyte determination factors and adipogenic genes were markedly inhibited by SOX4, whereas the proliferation genes and Wnt signaling molecules were activated in *Pref1-Sox4* mice, consistent with the preceding data (Figures 8B and 8C). Furthermore, to explore the role of SOX4 in transmitting BMP4 and TGFβ signaling and activating Wnt signaling *in vivo*, PDGFRα$^+$ cells were sorted from iWAT of WT and *Pref1-Sox4* mice and treated with BMP4 or SB431542. As shown in Figure 8D, both BMP4 and SB431542 inhibited the expression of *Sox4*, *Lef1*, and Wnt targets and improved the level of *Pparγ2*. However, the overexpression of SOX4 removed the effects of BMP4 and SB431542 and improved the levels of Wnt targets (Figure 8D).

To further confirm that the alteration of gene expression exerts cellular composition and phenotype changes, we isolated SVFs from HFD-fed WT and *Pref1-Sox4* mice and performed adipocyte differentiation *in vitro*. qPCR analysis showed that compared with WT group, *Pref1-Sox4* group had lower expression of adipogenic genes and higher levels of fibrogenesis genes (Figure 8E). Oil Red O staining revealed less lipid accumulation in the *Pref1-Sox4* group (Figure 8F), whereas Sirius Red staining showed more type I collagen fibers in this group (Figure 8G), which was consistent with the results observed *in vivo*.

At the molecular level, these findings suggested that SOX4 mediates crosstalk between the BMP4/TGFβ pathway and the Wnt signaling pathway, and regulates preadipocyte determination and WAT gene expression profiles *in vivo*.

## DISCUSSION

Preadipocyte determination expands the pool of preadipocytes and thus enhances the hyperplasia of adipocytes.[3,64] TGFβ and BMP4 signaling exerts antagonistic roles on this process. In this study, we identified SOX4 as the new intrinsic signaling molecule to control adipocyte hyperplasia by inhibiting preadipocyte determination. First, SOX4 functions as a pivotal mediator that controls the antagonistic actions of BMP4 and TGFβ on the preadipocyte determination of MSCs as TGFβ signaling activates SOX4 "switch on" to exert an inhibitory effect, while BMP4 signaling activates SOX4 "switch off" to initiate the preadipocyte determination. Second, SOX4 is highly expressed in MSCs rather than in preadipocytes. The deficiency of SOX4 in MSCs is sufficient to induce the expression of critical preadipocyte determinant PPARγ2 and a substantial proportion of preadipocyte genes, resulting in the determination of preadipocytes. Furthermore, specific overexpression of SOX4 in preadipocytes, a subpopulation emerged relatively late in fate determination, attenuated the preadipocyte determination, as manifested by the decreased proportion of preadipocytes and the increased proportion of earlier mesenchymal progenitors and adipocyte

progenitors in *Pref1-Sox4* transgenic mice. Collectively, these results provided evidence that the preadipocyte determination process can be controlled by altering the level of SOX4.

WAT is a large organ with multiple plastic properties to address specific physiological needs. For example, long-term cold stimulation induces browning, and chronic positive energy balance induces whitening. During pregnancy and lactation, "pink adipocytes" located in the breast subcutaneous WAT convert to secretory mammary glands.[65] Herein, we reported that the altered expression of SOX4 induces conversion between adipogenic and nonadipogenic lineages. First, nonadipogenic lineages, such as NIH3T3 and C2C12 with SOX4 deficiency, express a high level of PPARγ2 and acquire enhanced adipogenic potential. Second, the overexpression of SOX4 in highly adipogenic preadipocytes upregulates the levels of nonadipogenic-fibroblast gene profile both *in vitro* and *in vivo*. Moreover, *Pref1-Sox4* mice exhibited a significantly increased proportion of nonadipogenic stem cells in iWAT, and *in vitro* cultures of adipocyte precursors isolated from these mice demonstrated decreased lipid accumulation and increased fibrogenesis. These observations proposed that SOX4 regulates adipocyte hyperplasia by altering cellular plasticity, and these nonadipogenic lineages derived through transdifferentiation are the major contributors to extracellular matrix in the adipose compartment.[66]

Wnt/β-catenin signaling activation in adipocyte progenitors results in a severe loss of adiposity and induces fibrotic replacement of subcutaneous fat.[22] Conversely, its termination is necessary for adipose precursors to enter the adipose lineage.[20,67] The current study showed that SOX4-deficient MSCs display a reduced output level of Wnt/β-catenin and acquire adipogenic potential. We also highlighted that SOX4 bridges the TGFβ/BMP4 signaling and Wnt/β-catenin pathways in the preadipocyte determination program, as SOX4 overexpression eliminates the effects of BMP4 or SB431542 on the activity of Wnt/β-catenin signaling pathway. According to previous concepts, the transduction of Wnt signaling and the transactivation of Wnt targets depends on the subcellular localization of β-catenin, which shuttles between the cytoplasm and the nucleus via binding to various interaction partners.[14,68] A few Sox family factors have been demonstrated to emerge as the modulators of the Wnt/β-catenin signaling pathway, but the effect varies according to the individual subfamily member.[69–71] The current study revealed that LEF1 is the major Wnt transcription factor responsible for the inhibition of preadipocyte determination. Through binding to the regulatory elements adjacent to LEF1-binding sites, SOX4 cooperates with LEF1 to retain β-catenin in the nucleus, which is crucial for the transcriptional activation of *Lef1* as well as the Wnt targets. Collectively, these findings unravel the molecular mechanism of SOX4 in regulating the generation of preadipocytes and illuminating a model of SOX4-mediated activation of the Wnt/β-catenin signaling pathway.

During the embryonic development, adipocyte hyperplasia contributes to the expansion of WAT mass, while in obesity, it occurs when the upper limit on adipocyte size is achieved to enlarge the pool for excess energy storage. Since mature adipocytes are postmitotic, newly generated adipocytes are primarily differentiated from preadipocytes. The mesenchymal progenitors distributed in adipose tissues go through preadipocyte determination and provide an unlimited supply of preadipocytes. Previous studies have shown that HFD feeding in mice rapidly and transiently induces generation of adipocyte precursors within the WAT.[72] Our study also found that prolonged HFD induces the hyperplasia of preadipocytes, and SOX4 has the potential to inhibit this process. Therefore, it was necessary to construct a suitable mouse model to accurately drive SOX4 knockout in earlier MSCs (or progenitors) or overexpression in preadipocytes to test our hypothesis. PDGFRα-cre mouse is a well-known candidate model for genetic targeting of adipocyte precursor cells *in vivo*. However, this model has inherent limitations. For example, previous studies in iWAT demonstrated that PDGFRα$^+$ populations contain both preadipocytes and earlier interstitial progenitor cells.[60,73] suggesting that PDGFRα has less specificity in studies of preadipocyte determination targeting either mesenchymal progenitors or preadipocytes. In adipogenesis studies, *Pparγ* promoter was often used as a candidate to drive gene overexpression or deletion. However, the expression of PPARγ in both preadipocytes and adipocytes somewhat decreases the accuracy of targeting.[50,60] Pref1, on the other hand, first appeared as early as embryonic day 10.5 and was highly concentrated in the ICAM1$^+$ preadipocytes in 12-day-old (p12) mice, which was clearly confirmed by both single-cell RNA sequencing and tissue immunofluorescence.[8,54] Gulyaeva et al. have constructed a *Pref1*-driven conditional ablation mice model and demonstrated the *Pref1* promoter-rtTA system for inducible gene inactivation in preadipocytes.[55] Herein, we constructed *Pref1-Sox4* transgenic mice aiming to determine whether SOX4 overexpression inhibits the generation of primary preadipocytes *in vivo*. In HFD condition, SOX4 overexpression was highly induced in ICAM1$^+$ preadipocytes following a hyperactivation of *Pref1* gene, and protected mice from

HFD-induced adiposity. First, the overexpression of SOX4 inhibits adipocyte hyperplasia, mainly by impeding the preadipocyte determination while boosting transdifferentiation toward nonadipogenic lineages. Second, SOX4 impairs the adipogenic potential of preadipocytes by inhibiting the expression of adipogenic genes, which at least partially suppresses the hypertrophy of white adipocytes. During normal feeding, however, these inhibitory effects were mild. We speculated that this was due to the lower efficiency of SOX4 overexpression.

In summary, the current study revealed the role and molecular mechanism of SOX4 in inhibiting preadipocyte determination and hyperplasia of white adipose tissues, providing a potential therapeutic target or strategy for treating obesity. Besides, given the possibility of isolation and *in vitro* culture of human MSCs, this study opens possibilities for extracorporeal fat reconstruction and clinical applications, whether in regenerative surgery or medical cosmetic applications.

### Limitations of the study

In this study, in addition to the inhibition of adipocyte proliferation, we observed that the size of white adipocytes decreased in *Pref1-Sox4* mice fed with NCD or HFD for 20 weeks. Also, these mice were protected from HFD-induced glucose intolerance and insulin resistance, which means dual suppression of hyperplasia and hypertrophy protects *Pref1-Sox4* mice from diet-induced obesity without causing maladaptive metabolic response. Based on this observation and previous studies aforementioned,[7,57] we speculate that SOX4 plays a role in energy metabolism, which requires further investigation. Moreover, since adipocyte hyperplasia and hypertrophy have been proposed to play a significant role in the pathogenesis of metabolic disease, more efforts should be made to establish the model of human obesity and metabolic disease to verify the role of SOX4.

## STAR★METHODS

Detailed methods are provided in the online version of this paper and include the following:

- KEY RESOURCES TABLE
- RESOURCE AVAILABILITY
  - Lead contact
  - Materials availability
  - Data and code availability
- EXPERIMENTAL MODEL AND SUBJECT DETAILS
  - Cell lines
  - Mouse model
- METHOD DETAILS
  - Body weight, body composition, and blood analysis
  - H&E staining and Sirius red staining
  - *In vitro* adipogenesis
  - Immunofluorescence
  - Isolation of SVFs and adipocytes, DNA quantification and flow cytometry
  - Oil Red O staining and Nile Red staining
  - Chromatin immunoprecipitation assay (ChIP)
  - Co-immunoprecipitation (CoIP)
  - GST pull-down
  - Luciferase reporter assay
  - Quantitative real-time PCR (qPCR) and western blot
  - Plasmids, production of lentivirus and lentivirus-mediated gene transfer
- QUANTIFICATION AND STATISTICAL ANALYSIS

## SUPPLEMENTAL INFORMATION

Supplemental information can be found online at https://doi.org/10.1016/j.isci.2023.106289.

## ACKNOWLEDGMENTS

This work was supported by grants from the National Key Research and Development Program of China (2020YFA0112300 to B.-A.L.), the National Natural Science Foundation of China (grant number 81972458

to B.-A.L. 82103092 to R.Z.), the Natural Science Foundation of Fujian Province (grant number 2022J05312 to R.Z.) the Health-Education joint research project of Fujian province (grant numbers 2019-WJ-34 to B.-A.L. and Z.-M.Z.), and "Project 111" sponsored by the State Bureau of Foreign Experts and Ministry of Education (grant number B06016).

## AUTHOR CONTRIBUTIONS

T.H. designed and carried out overall experiments and wrote the paper. S.W., H.-M.S., and L.-F.H. performed experiments, analyzed, and interpreted data. S.-N.L. designed the experiments and analyzed data. Y.-J.L., Y.-X.W., Z.-H.Z., C.-L.M., and Q.-S.H. assisted with mouse experiments and data analysis. H.-L.G., F.-A.X., and Z.-M.Z. proofread the manuscripts and provided modification suggestions. B.-A.L., D.-Y.S., and R.Z. supervised the project and revised the manuscript. B.-A.L. is the guarantor of this work and, as such, had full access to all the data in the study and takes responsibility for the integrity of the data and the accuracy of the data analysis.

## DECLARATION OF INTERESTS

The authors declare no competing interests.

## INCLUSION AND DIVERSITY

We support inclusive, diverse, and equitable conduct of research.

Received: September 29, 2022
Revised: January 3, 2023
Accepted: February 20, 2023
Published: February 28, 2023

## REFERENCES

1. Tinahones, F.J., Coín-Aragüez, L., Mayas, M.D., Garcia-Fuentes, E., Hurtado-Del-Pozo, C., Vendrell, J., Cardona, F., Calvo, R.M., Obregon, M.J., and El Bekay, R. (2012). Obesity-associated insulin resistance is correlated to adipose tissue vascular endothelial growth factors and metalloproteinase levels. BMC Physiol. *12*, 4. https://doi.org/10.1186/1472-6793-12-4.

2. Gaesser, G.A., and Angadi, S.S. (2021). Obesity treatment: weight loss versus increasing fitness and physical activity for reducing health risks. iScience *24*, 102995. https://doi.org/10.1016/j.isci.2021.102995.

3. Tang, Q.Q., and Lane, M.D. (2012). Adipogenesis: from stem cell to adipocyte. Annu. Rev. Biochem. *81*, 715–736. https://doi.org/10.1146/annurev-biochem-052110-115718.

4. Haider, N., Dusseault, J., and Larose, L. (2018). Nck1 deficiency impairs adipogenesis by activation of PDGFRα in preadipocytes. iScience *6*, 22–37. https://doi.org/10.1016/j.isci.2018.07.010.

5. Luo, L., and Liu, M. (2016). Adipose tissue in control of metabolism. J. Endocrinol. *231*, R77–R99. https://doi.org/10.1530/joe-16-0211.

6. Cristancho, A.G., and Lazar, M.A. (2011). Forming functional fat: a growing understanding of adipocyte differentiation. Nat. Rev. Mol. Cell Biol. *12*, 722–734. https://doi.org/10.1038/nrm3198.

7. Muir, L.A., Neeley, C.K., Meyer, K.A., Baker, N.A., Brosius, A.M., Washabaugh, A.R., Varban, O.A., Finks, J.F., Zamarron, B.F., Flesher, C.G., et al. (2016). Adipose tissue fibrosis, hypertrophy, and hyperplasia: correlations with diabetes in human obesity. Obesity *24*, 597–605. https://doi.org/10.1002/oby.21377.

8. Merrick, D., Sakers, A., Irgebay, Z., Okada, C., Calvert, C., Morley, M.P., Percec, I., and Seale, P. (2019). Identification of a mesenchymal progenitor cell hierarchy in adipose tissue. Science *364*, eaav2501. https://doi.org/10.1126/science.aav2501.

9. Moerman, E.J., Teng, K., Lipschitz, D.A., and Lecka-Czernik, B. (2004). Aging activates adipogenic and suppresses osteogenic programs in mesenchymal marrow stroma/stem cells: the role of PPAR-gamma2 transcription factor and TGF-beta/BMP signaling pathways. Aging Cell *3*, 379–389. https://doi.org/10.1111/j.1474-9728.2004.00127.x.

10. Modica, S., and Wolfrum, C. (2017). The dual role of BMP4 in adipogenesis and metabolism. Adipocyte *6*, 141–146. https://doi.org/10.1080/21623945.2017.1287637.

11. Huang, H., Song, T.-J., Li, X., Hu, L., He, Q., Liu, M., Lane, M.D., and Tang, Q.-Q. (2009). BMP signaling pathway is required for commitment of C3H10T1/2 pluripotent stem cells to the adipocyte lineage. Proc. Natl. Acad. Sci. USA *106*, 12670–12675. https://doi.org/10.1073/pnas.0906266106.

12. Tang, Q.Q., Otto, T.C., and Lane, M.D. (2004). Commitment of C3H10T1/2 pluripotent stem cells to the adipocyte lineage. Proc. Natl. Acad. Sci. USA *101*, 9607–9611. https://doi.org/10.1073/pnas.0403100101.

13. Bowers, R.R., Kim, J.W., Otto, T.C., and Lane, M.D. (2006). Stable stem cell commitment to the adipocyte lineage by inhibition of DNA methylation: role of the BMP-4 gene. Proc. Natl. Acad. Sci. USA *103*, 13022–13027. https://doi.org/10.1073/pnas.0605789103.

14. Krieghoff, E., Behrens, J., and Mayr, B. (2006). Nucleo-cytoplasmic distribution of beta-catenin is regulated by retention. J. Cell Sci. *119*, 1453–1463. https://doi.org/10.1242/jcs.02864.

15. Longo, K.A., Wright, W.S., Kang, S., Gerin, I., Chiang, S.H., Lucas, P.C., Opp, M.R., and MacDougald, O.A. (2004). Wnt10b inhibits development of white and brown adipose tissues. J. Biol. Chem. *279*, 35503–35509. https://doi.org/10.1074/jbc.M402937200.

16. Kanazawa, A., Tsukada, S., Sekine, A., Tsunoda, T., Takahashi, A., Kashiwagi, A., Tanaka, Y., Babazono, T., Matsuda, M., Kaku, K., et al. (2004). Association of the gene encoding wingless-type mammary tumor virus integration-site family member 5B (WNT5B) with type 2 diabetes. Am. J. Hum. Genet. *75*, 832–843. https://doi.org/10.1086/425340.

17. Christodoulides, C., Scarda, A., Granzotto, M., Milan, G., Dalla Nora, E., Keogh, J., De Pergola, G., Stirling, H., Pannacciulli, N., Sethi, J.K., et al. (2006). WNT10B mutations in

human obesity. Diabetologia *49*, 678–684. https://doi.org/10.1007/s00125-006-0144-4.

18. Wang, J., Liu, R., Wang, F., Hong, J., Li, X., Chen, M., Ke, Y., Zhang, X., Ma, Q., Wang, R., et al. (2013). Ablation of LGR4 promotes energy expenditure by driving white-to-brown fat switch. Nat. Cell Biol. *15*, 1455–1463. https://doi.org/10.1038/ncb2867.

19. Mattei, J., Qi, Q., Hu, F.B., Sacks, F.M., and Qi, L. (2012). TCF7L2 genetic variants modulate the effect of dietary fat intake on changes in body composition during a weight-loss intervention. Am. J. Clin. Nutr. *96*, 1129–1136. https://doi.org/10.3945/ajcn.112.038125.

20. Ross, S.E., Hemati, N., Longo, K.A., Bennett, C.N., Lucas, P.C., Erickson, R.L., and MacDougald, O.A. (2000). Inhibition of adipogenesis by Wnt signaling. Science *289*, 950–953. https://doi.org/10.1126/science.289.5481.950.

21. Xie, Y.Y., Mo, C.L., Cai, Y.H., Wang, W.J., Hong, X.X., Zhang, K.K., Liu, Q.F., Liu, Y.J., Hong, J.J., He, T., et al. (2018). Pygo2 regulates adiposity and glucose homeostasis via beta-catenin-Axin2-GSK3beta signaling pathway. Diabetes *67*, 2569–2584. https://doi.org/10.2337/db18-0311.

22. Zeve, D., Seo, J., Suh, J.M., Stenesen, D., Tang, W., Berglund, E.D., Wan, Y., Williams, L.J., Lim, A., Martinez, M.J., et al. (2012). Wnt signaling activation in adipose progenitors promotes insulin-independent muscle glucose uptake. Cell Metab. *15*, 492–504. https://doi.org/10.1016/j.cmet.2012.03.010.

23. Bowles, J., Schepers, G., and Koopman, P. (2000). Phylogeny of the SOX family of developmental transcription factors based on sequence and structural indicators. Dev. Biol. *227*, 239–255. https://doi.org/10.1006/dbio.2000.9883.

24. Vervoort, S.J., van Boxtel, R., and Coffer, P.J. (2013). The role of SRY-related HMG box transcription factor 4 (SOX4) in tumorigenesis and metastasis: friend or foe? Oncogene *32*, 3397–3409. https://doi.org/10.1038/onc.2012.506.

25. Schilham, M.W., Oosterwegel, M.A., Kruisbeek, A.M., Cumano, A., Clevers, H., Moerer, P., Ya, J., de Boer, P.A.J., van de Wetering, M., Verbeek, S., and Lamers, W.H. (1996). Defects in cardiac outflow tract formation and pro-B-lymphocyte expansion in mice lacking Sox4. Nature *380*, 711–714.

26. Dy, P., Penzo-Méndez, A., Wang, H., Pedraza, C.E., Macklin, W.B., and Lefebvre, V. (2008). The three SoxC proteins–Sox4, Sox11 and Sox12–exhibit overlapping expression patterns and molecular properties. Nucleic Acids Res. *36*, 3101–3117. https://doi.org/10.1093/nar/gkn162.

27. Nissen-Meyer, L.S.H., Jemtland, R., Gautvik, V.T., Pedersen, M.E., Paro, R., Fortunati, D., Pierroz, D.D., Stadelmann, V.A., Reppe, S., Reinholt, F.P., et al. (2007). Osteopenia, decreased bone formation and impaired osteoblast development in Sox4 heterozygous mice. J. Cell Sci. *120*, 2785–2795. https://doi.org/10.1242/jcs.003855.

28. Lioubinski, O., Müller, M., Wegner, M., and Sander, M. (2003). Expression of Sox transcription factors in the developing mouse pancreas. Dev. Dyn. *227*, 402–408. https://doi.org/10.1002/dvdy.10311.

29. Van der Flier, L.G., Sabates-Bellver, J., Oving, I., Haegebarth, A., De Palo, M., Anti, M., Van Gijn, M.E., Suijkerbuijk, S., Van de Wetering, M., Marra, G., and Clevers, H. (2007). The intestinal Wnt/TCF signature. Gastroenterology *132*, 628–632. https://doi.org/10.1053/j.gastro.2006.08.039.

30. Deneault, E., Cellot, S., Faubert, A., Laverdure, J.P., Fréchette, M., Chagraoui, J., Mayotte, N., Sauvageau, M., Ting, S.B., and Sauvageau, G. (2009). A functional screen to identify novel effectors of hematopoietic stem cell activity. Cell *137*, 369–379. https://doi.org/10.1016/j.cell.2009.03.026.

31. Pece, S., Tosoni, D., Confalonieri, S., Mazzarol, G., Vecchi, M., Ronzoni, S., Bernard, L., Viale, G., Pelicci, P.G., and Di Fiore, P.P. (2010). Biological and molecular heterogeneity of breast cancers correlates with their cancer stem cell content. Cell *140*, 62–73. https://doi.org/10.1016/j.cell.2009.12.007.

32. Lourenço, A.R., and Coffer, P.J. (2017). SOX4: joining the master regulators of epithelial-to-mesenchymal transition? Trends Cancer *3*, 571–582. https://doi.org/10.1016/j.trecan.2017.06.002.

33. Ross, S., Cheung, E., Petrakis, T.G., Howell, M., Kraus, W.L., and Hill, C.S. (2006). Smads orchestrate specific histone modifications and chromatin remodeling to activate transcription. EMBO J. *25*, 4490–4502. https://doi.org/10.1038/sj.emboj.7601332.

34. David, C.J., Huang, Y.-H., Chen, M., Su, J., Zou, Y., Bardeesy, N., Iacobuzio-Donahue, C.A., and Massagué, J. (2016). TGF-β tumor suppression through a lethal EMT. Cell *164*, 1015–1030. https://doi.org/10.1016/j.cell.2016.01.009.

35. Marcelin, G., Silveira, A.L.M., Martins, L.B., Ferreira, A.V., and Clément, K. (2019). Deciphering the cellular interplays underlying obesity-induced adipose tissue fibrosis. J. Clin. Invest. *129*, 4032–4040. https://doi.org/10.1172/jci129192.

36. Gupta, R.K., Arany, Z., Seale, P., Mepani, R.J., Ye, L., Conroe, H.M., Roby, Y.A., Kulaga, H., Reed, R.R., and Spiegelman, B.M. (2010). Transcriptional control of preadipocyte determination by Zfp423. Nature *464*, 619–623. https://doi.org/10.1038/nature08816.

37. Chen, Q., Shou, P., Zheng, C., Jiang, M., Cao, G., Yang, Q., Cao, J., Xie, N., Velletri, T., Zhang, X., et al. (2016). Fate decision of mesenchymal stem cells: adipocytes or osteoblasts? Cell Death Differ. *23*, 1128–1139. https://doi.org/10.1038/cdd.2015.168.

38. Hammarstedt, A., Hedjazifar, S., Jenndahl, L., Gogg, S., Grünberg, J., Gustafson, B., Klimcakova, E., Stich, V., Langin, D., Laakso, M., and Smith, U. (2013). WISP2 regulates preadipocyte commitment and PPARγ activation by BMP4. Proc. Natl. Acad. Sci. USA *110*, 2563–2568. https://doi.org/10.1073/pnas.1211255110.

39. Li, S.N., and Wu, J.F. (2020). TGF-β/SMAD signaling regulation of mesenchymal stem cells in adipocyte commitment. Stem Cell Res. Ther. *11*, 41. https://doi.org/10.1186/s13287-020-1552-y.

40. Massagué, J. (2012). TGFβ signalling in context. Nat. Rev. Mol. Cell Biol. *13*, 616–630. https://doi.org/10.1038/nrm3434.

41. Katoh, M., and Katoh, M. (2007). WNT signaling pathway and stem cell signaling network. Clin. Cancer Res. *13*, 4042–4045. https://doi.org/10.1158/1078-0432.CCR-06-2316.

42. Du, M., Yin, J., and Zhu, M.J. (2010). Cellular signaling pathways regulating the initial stage of adipogenesis and marbling of skeletal muscle. Meat Sci. *86*, 103–109. https://doi.org/10.1016/j.meatsci.2010.04.027.

43. Ng, F., Boucher, S., Koh, S., Sastry, K.S.R., Chase, L., Lakshmipathy, U., Choong, C., Yang, Z., Vemuri, M.C., Rao, M.S., and Tanavde, V. (2008). PDGF, TGF-and FGF signaling is important for differentiation and growth of mesenchymal stem cells (MSCs): transcriptional profiling can identify markers and signaling pathways important in differentiation of MSCs into adipogenic, chondrogenic, and osteogenic lineages. Blood *112*, 295–307. https://doi.org/10.1182/blood-2007-07-103697.

44. Ahmadian, M., Suh, J.M., Hah, N., Liddle, C., Atkins, A.R., Downes, M., and Evans, R.M. (2013). PPARgamma signaling and metabolism: the good, the bad and the future. Nat. Med. *19*, 557–566. https://doi.org/10.1038/nm.3159.

45. Clevers, H., and Nusse, R. (2012). Wnt/β-catenin signaling and disease. Cell *149*, 1192–1205. https://doi.org/10.1016/j.cell.2012.05.012.

46. De Sousa E Melo, F., and Medema, J.P. (2012). Axing Wnt signals. Cell Res. *22*, 9–11. https://doi.org/10.1038/cr.2011.141.

47. Cai, W.Y., Wei, T.Z., Luo, Q.C., Wu, Q.W., Liu, Q.F., Yang, M., Ye, G.D., Wu, J.F., Chen, Y.Y., Sun, G.B., et al. (2013). The Wnt-β-catenin pathway represses let-7 microRNA expression through transactivation of Lin28 to augment breast cancer stem cell expansion. J. Cell Sci. *126*, 2877–2889. https://doi.org/10.1242/jcs.123810.

48. MacDonald, B.T., Tamai, K., and He, X. (2009). Wnt/beta-catenin signaling: components, mechanisms, and diseases. Dev. Cell *17*, 9–26. https://doi.org/10.1016/j.devcel.2009.06.016.

49. Law, S.M., and Zheng, J.J. (2022). Premise and peril of Wnt signaling activation through GSK-3β inhibition. iScience *25*, 104159. https://doi.org/10.1016/j.isci.2022.104159.

50. Tang, W., Zeve, D., Suh, J.M., Bosnakovski, D., Kyba, M., Hammer, R.E., Tallquist, M.D., and Graff, J.M. (2008). White fat progenitor cells reside in the adipose vasculature.

Science *322*, 583–586. https://doi.org/10.1126/science.1156232.

51. Hepler, C., Vishvanath, L., and Gupta, R.K. (2017). Sorting out adipocyte precursors and their role in physiology and disease. Genes Dev. *31*, 127–140. https://doi.org/10.1101/gad.293704.

52. Wang, W., and Seale, P. (2016). Control of brown and beige fat development. Nat. Rev. Mol. Cell Biol. *17*, 691–702. https://doi.org/10.1038/nrm.2016.96.

53. Hudak, C.S., and Sul, H.S. (2013). Pref-1, a gatekeeper of adipogenesis. Front. Endocrinol. *4*, 79. https://doi.org/10.3389/fendo.2013.00079.

54. Hudak, C.S., Gulyaeva, O., Wang, Y., Park, S.-M., Lee, L., Kang, C., and Sul, H.S. (2014). Pref-1 marks very early mesenchymal precursors required for adipose tissue development and expansion. Cell Rep. *8*, 678–687. https://doi.org/10.1016/j.celrep.2014.06.060.

55. Gulyaeva, O., Nguyen, H., Sambeat, A., Heydari, K., and Sul, H.S. (2018). Sox9-Meis1 inactivation is required for adipogenesis, advancing Pref-1(+) to PDGFRalpha(+) cells. Cell Rep. *25*, 1002–1017.e4. https://doi.org/10.1016/j.celrep.2018.09.086.

56. Wang, Q.A., Tao, C., Gupta, R.K., and Scherer, P.E. (2013). Tracking adipogenesis during white adipose tissue development, expansion and regeneration. Nat. Med. *19*, 1338–1344. https://doi.org/10.1038/nm.3324.

57. Shen, H., He, T., Wang, S., Hou, L., Wei, Y., Liu, Y., Mo, C., Zhao, Z., You, W., Guo, H., and Li, B. (2022). SOX4 promotes beige adipocyte-mediated adaptive thermogenesis by facilitating PRDM16-PPARγ complex. Theranostics *12*, 7699–7716. https://doi.org/10.7150/thno.77102.

58. Rodeheffer, M.S., Birsoy, K., and Friedman, J.M. (2008). Identification of white adipocyte progenitor cells in vivo. Cell *135*, 240–249. https://doi.org/10.1016/j.cell.2008.09.036.

59. Mohsen-Kanson, T., Hafner, A.L., Wdziekonski, B., Villageois, P., Chignon-Sicard, B., and Dani, C. (2013). Expression of cell surface markers during self-renewal and differentiation of human adipose-derived stem cells. Biochem. Biophys. Res. Commun. *430*, 871–875. https://doi.org/10.1016/j.bbrc.2012.12.079.

60. Berry, R., Jeffery, E., and Rodeheffer, M.S. (2014). Weighing in on adipocyte precursors. Cell Metab. *19*, 8–20. https://doi.org/10.1016/j.cmet.2013.10.003.

61. Church, C., Brown, M., and Rodeheffer, M.S. (2015). Conditional immortalization of primary adipocyte precursor cells. Adipocyte *4*, 203–211. https://doi.org/10.1080/21623945.2014.995510.

62. Berry, R., and Rodeheffer, M.S. (2013). Characterization of the adipocyte cellular lineage in vivo. Nat. Cell Biol. *15*, 302–308. https://doi.org/10.1038/ncb2696.

63. Berry, R., Rodeheffer, M.S., Rosen, C.J., and Horowitz, M.C. (2015). Adipose tissue residing progenitors (adipocyte lineage progenitors and adipose derived stem cells (ADSC). Curr. Mol. Biol. Rep. *1*, 101–109. https://doi.org/10.1007/s40610-015-0018-y.

64. Schneider, M.K., Xue, B., and Shi, H. (2018). Activation of the sympathetic nervous system suppresses mouse white adipose tissue hyperplasia through the β1 adrenergic receptor. Physiol. Rep. *6*, e13645. https://doi.org/10.14814/phy2.13645.

65. Cinti, S. (2018). Pink adipocytes. Trends Endocrinol. Metab. *29*, 651–666. https://doi.org/10.1016/j.tem.2018.05.007.

66. Datta, R., Podolsky, M.J., and Atabai, K. (2018). Fat fibrosis: friend or foe? JCI Insight *3*, e122289. https://doi.org/10.1172/jci.insight.122289.

67. Christodoulides, C., Lagathu, C., Sethi, J.K., and Vidal-Puig, A. (2009). Adipogenesis and WNT signalling. Trends Endocrinol. Metab. *20*, 16–24. https://doi.org/10.1016/j.tem.2008.09.002.

68. Zhang, Z.M., Wu, J.F., Luo, Q.C., Liu, Q.F., Wu, Q.W., Ye, G.D., She, H.Q., and Li, B.A. (2016). Pygo2 activates MDR1 expression and mediates chemoresistance in breast cancer via the Wnt/β-catenin pathway. Oncogene *35*, 4787–4797. https://doi.org/10.1038/onc.2016.10.

69. Bhattaram, P., Penzo-Méndez, A., Kato, K., Bandyopadhyay, K., Gadi, A., Taketo, M.M., and Lefebvre, V. (2014). SOXC proteins amplify canonical WNT signaling to secure nonchondrocytic fates in skeletogenesis. J. Cell Biol. *207*, 657–671. https://doi.org/10.1083/jcb.201405098.

70. Sinner, D., Kordich, J.J., Spence, J.R., Opoka, R., Rankin, S., Lin, S.C.J., Jonatan, D., Zorn, A.M., and Wells, J.M. (2007). Sox17 and Sox4 differentially regulate beta-catenin/T-cell factor activity and proliferation of colon carcinoma cells. Mol. Cell Biol. *27*, 7802–7815. https://doi.org/10.1128/MCB.02179-06.

71. Kormish, J.D., Sinner, D., and Zorn, A.M. (2010). Interactions between SOX factors and Wnt/beta-catenin signaling in development and disease. Dev. Dyn. *239*, 56–68. https://doi.org/10.1002/dvdy.22046.

72. Jeffery, E., Church, C.D., Holtrup, B., Colman, L., and Rodeheffer, M.S. (2015). Rapid depot-specific activation of adipocyte precursor cells at the onset of obesity. Nat. Cell Biol. *17*, 376–385. https://doi.org/10.1038/ncb3122.

73. Joe, A.W.B., Yi, L., Natarajan, A., Le Grand, F., So, L., Wang, J., Rudnicki, M.A., and Rossi, F.M.V. (2010). Muscle injury activates resident fibro/adipogenic progenitors that facilitate myogenesis. Nat. Cell Biol. *12*, 153–163. https://doi.org/10.1038/ncb2015.

## STAR★METHODS

### KEY RESOURCES TABLE

| REAGENT or RESOURCE | SOURCE | IDENTIFIER |
|---|---|---|
| Antibodies | | |
| Rabbit polyclonal anti-Sox4 | Sigma | Cat#AV-38234; RRID: AB_1857386 |
| Mouse monoclonal anti-Sox4 | Abcam | Cat#ab70598; RRID: AB_1270867 |
| Mouse polyclonal anti-Sox4 | Millipore | Cat#AB10537; RRID: AB_10806202 |
| Rabbit monoclonal anti-β-catenin | CST | Cat#8480S; RRID: AB_11127855 |
| Rabbit polyclonal anti-Phospho-β-catenin | CST | Cat#9561; RRID: AB_331729 |
| Mouse monoclonal anti-Lef1 | CST | Cat#2286; RRID: AB_659971 |
| Mouse polyclonal anti-Lef1 | Proteintech | Cat#14972-1-AP; RRID:AB_2265677 |
| Rabbit polyclonal anti–TCF1 | Proteintech | Cat#14464-1-AP; RRID: AB_2878061 |
| Rabbit polyclonal anti–TCF3 | Proteintech | Cat#14519-1-AP; RRID: AB_2287033 |
| Rabbit polyclonal anti–TCF4 | Proteintech | Cat#22337-1-AP; RRID: AB_2879076 |
| Rabbit monoclonal anti-AXIN2 | Abcam | Cat#Ab109307; RRID:AB_10862550 |
| Rabbit polyclonal anti-FABP4 | Proteintech | Cat#12802-1-AP; RRID: AB_2102442 |
| Rabbit polyclonal anti-PPARγ2 | Proteintech | Cat#16643-1-AP; RRID: AB_10596794 |
| Rabbit polyclonal anti-C/EBPα | Santa Cruz | Cat#SC-61; RRID: AB_631233 |
| Rabbit polyclonal anti-C/EBPβ | Santa Cruz | Cat#SC-150; RRID: AB_2260363 |
| Rabbit polyclonal anti-ZFP423 | Abcam | Cat#ab94451; RRID: AB_10672707 |
| Rabbit monoclonal anti-SMAD2 | CST | Cat#5339; RRID: AB_10626777 |
| Mouse monoclonal anti-β-actin | Sigma-Aldrich | Cat#A1978; RRID: AB_476692 |
| Goat polyclonal anti-LaminB | Santa Cruz | Cat#SC-6216; RRID: AB_648156 |
| Mouse Monoclonal anti-C-Myc | Sigma | Cat#ZMS1032 |
| Mouse anti-His-Tag | abclonal | Cat#AE003; RRID: AB_2728734 |
| Rabbit polyclonal anti-Flag | Sigma-Aldrich | Cat#F7425; RRID: AB_439687 |
| Mouse Monoclonal anti-GAPDH | Sigma-Aldrich | Cat#G9295; RRID: AB_1078992 |
| CD45 Monoclonal Antibody (30-F11), APC-eFluor™ 780 | eBioscience | Cat#47-0451-80; RRID: AB_1548790 |
| CD45.1 Monoclonal Antibody (A20), PE-Cyanine7 | eBioscience | Cat#25-0453-82; RRID: AB_469629 |
| CD31 (PECAM-1) Monoclonal Antibody (390), PE-Cyanine7 | eBioscience | Cat#25-0311-82; RRID: AB_2716949 |
| PE/Cyanine7 anti-mouse CD31 | Biolegend | Cat#102524; RRID: AB_2572182 |
| TER-119 Monoclonal Antibody (TER-119), PE | eBioscience | Cat#12-5921-82; RRID: AB_466042 |
| PE/Cyanine7 anti-mouse TER-119 | Biolegend | Cat#116221; RRID: AB_2137789 |
| Alexa Fluor® 700 anti-mouse/rat CD29 | BioLegend | Cat#102218; RRID: AB_493711 |
| Alexa Fluor® 647 anti-mouse CD34 | BioLegend | Cat#119314; RRID: AB_604089 |
| V450 Rat Anti-Mouse Ly-6A/E (Sca-1) | BD Biosciences | Cat#560653; RRID: AB_1727553 |
| CD24 Monoclonal Antibody (M1/69), PerCP-Cyanine5.5 | eBioscience | Cat#45-0242-82; RRID: AB_1210701 |
| PE anti-mouse CD140a (PDGFRα) | BioLegend | Cat#135905; RRID: AB_1953268 |
| PE/Cyanine7 anti-mouse CD26 (DPP-4) | Biolegend | Cat#137810; RRID:AB_2564312 |
| BV421 Hamster Anti-Mouse CD54 (ICAM1) 3E2 | BD Biosciences | Cat#564704; RRID:AB_2738903 |
| Bacterial and virus strains | | |
| pLV-EF1A-Sox4 lentivirus | This paper | N/A |
| pLKO.1-Sox4 lentivirus | This paper | N/A |
| pLKO.1-Lef1 lentivirus | This paper | N/A |

(*Continued on next page*)

*Continued*

| REAGENT or RESOURCE | SOURCE | IDENTIFIER |
|---|---|---|
| pLV-Lef1 lentivirus | This paper | N/A |
| pMSCV-Sox4 retrovirus | This paper | N/A |
| pLKO.1-Tcf1 lentivirus | This paper | N/A |
| pLKO.1-Tcf3 lentivirus | This paper | N/A |
| pLKO.1-Tcf4 lentivirus | This paper | N/A |
| **Chemicals, peptides, and recombinant proteins** | | |
| BMP4 protein | R&D | Cat#5020-BP-010 |
| SB431542 | Sigma-Aldrich | Cat#S4317 |
| TGFβ1 | MCE | Cat#HY-P78360 |
| *Smad2* siRNA_1 | RIBBIO | Cat#SiB1096161142-1-5 |
| *Smad2* siRNA_2 | RIBBIO | Cat#SiB1096161154-1-5 |
| DAPI | Beyotime | Cat#C1002 |
| Type II collagenase | Sigma | Cat#C6885 |
| DNA Transfectin 3000 | Herogen Biotech | Cat#TS3000 |
| polyethylenimine | Polysciences | Cat#23966-1 |
| Turbofect | Themo | Cat#R0531 |
| Dexamethasone | Sigma-Aldrich | Cat#D1756 |
| IBMX | Sigma-Aldrich | Cat#I5879 |
| Insulin (human) | MCE | Cat#HY-P0035 |
| Rosiglitazone | MCE | Cat#HY-17386 |
| IP lysis buffer | Beyotime | Cat#P0013 |
| **Critical commercial assays** | | |
| hematoxylin-eosin kit | Boster | Cat#AR1180 |
| ChIP Assay Kit | Beyotime | Cat#P2078 |
| 5× All in One kit | Abm | Cat#G490 |
| BCA assay kit | Thermo Scientific | Cat#23227 |
| **Experimental models: Cell lines** | | |
| Mouse: C3H10T1/2 cell | Laboratory of Qi-qun Tang; Huang et al. 2009[11] | N/A |
| Mouse: 3T3-L1 cell | Laboratory of Qi-qun Tang; Huang et al. 2009[11] | N/A |
| Mouse: NIH3T3 | ATCC | Cat#CRL-1658 |
| Mouse: C2C12 | ATCC | Cat#CRL-1772 |
| Human: HEK 293T cells | ATCC | Cat# CRL-3216 |
| **Experimental models: Organisms/strains** | | |
| Mouse: Pref1-Sox4: C57BL/6-TgSox4 | This paper; Shen et al. 2022[61] | N/A |
| **Oligonucleotides** | | |
| Primers for ChIP assays, see Table S1 | This paper | N/A |
| Primers for qPCR, see Table S2 | This paper | N/A |
| shRNA targeting sequences, see Table S3 | This paper | N/A |
| Primers for construction of luciferase reporters, see Table S4 | This paper | N/A |
| **Recombinant DNA** | | |
| pLV-Flag-Lef1 plasmid | This paper | N/A |
| mCherry-β-catenin plasmid | This paper | N/A |
| pLV-EF1A-Sox4 plasmid | This paper | N/A |
| pGEX-4T3-Sox4 plasmid | This paper | N/A |

(*Continued on next page*)

*Continued*

| REAGENT or RESOURCE | SOURCE | IDENTIFIER |
|---|---|---|
| pGEX-4T3-β-catenin plasmid | This paper | N/A |
| pET-21b-Sox4 plasmid | This paper | N/A |
| pET-21b-Lef1 plasmid | This paper | N/A |
| pLV-HA-β-catenin (S33Y) | This paper | N/A |
| pLV-N-Flag-Sox4 | This paper | N/A |
| Software and algorithms | | |
| ImageJ_v1.8.0 | ImageJ, NIH | https://imagej.net/ij/download.html |
| GraphPad Prism 8.3.0 | GraphPad Software, LLC | https://www.graphpad.com/ |
| FlowJo v10.5.3 | BD Biosciences | https://www.flowjo.com/ |
| Other | | |
| High-fat diet | Research Diets | Cat#D12492i |
| Protein A/G magnetic beads | MCE | Cat#HY-K0202 |
| Centrifugal filter units (100 KDa) | Millipore | Cat#UFC910096 |

## RESOURCE AVAILABILITY

### Lead contact

Further information should be directed to and will be fulfilled by the lead contact, Boan Li (bali@xmu.edu.cn).

### Materials availability

All plasmids and mouse line generated in this study are available from the lead contact with a completed materials transfer agreement.

### Data and code availability

All data reported in this paper will be shared by the lead contact upon request.

This paper does not report original code.

Any additional information required to reanalyze the data reported in this paper is available from the lead contact upon request.

## EXPERIMENTAL MODEL AND SUBJECT DETAILS

### Cell lines

The C3H10T1/2 MSCs and 3T3-L1 preadipocytes were kindly donated by Qi-Qun Tang, Fudan University Shanghai Medical College. The C2C12 myoblasts, NIH3T3 fibroblasts and HEK 293T cells were purchased from the American Type Culture Collection (ATCC). All cell lines were routinely tested negative for mycoplasma contamination. The C3H10T1/2 MSCs and 3T3-L1 preadipocytes were cultured in growth media containing high-glucose DMEM, 1% penicillin/streptomycin and 10% FBS (Gibco) at 10% $CO_2$, 37 °C. C2C12 myoblasts and NIH3T3 fibroblasts were cultured in 5% $CO_2$ at 37 °C. WAT SVFs were maintained in high-glucose DMEM, 1% penicillin/streptomycin and 20% FBS at 10% $CO_2$, 37 °C.

### Mouse model

*Pref1-Sox4* mice were generated at Cyagen Company by inserting full-length mouse *Sox4* cDNA directly after 6 kb of the *Pref1* promoter in C57BL/6 mice. Male mice were used for all experiments. Littermates were randomly assigned to experimental groups. All mice were maintained in pathogen-free animal cages at 22 °C with a 12-h light/dark cycle (with light from 7:00 to 19:00). A high-fat diet or normal chow diet and water were provided *ad libitum*. All animal experiments were approved by the Institutional Animal Care and Use Committee of Xiamen University. And all the animals' care and use were in accordance with the National Institutes of Health guidelines.

## METHOD DETAILS

### Body weight, body composition, and blood analysis

Body weight was monitored weekly for 14 weeks. Body composition was measured with an NMR body composition analyzer (EchoMRI-100H, EchoMRI LLC, Houston, USA) after HFD feeding for 14 weeks. For the glucose tolerance test (GTT), mice fed with NCD or HFD for 20 weeks were injected intraperitoneally with glucose at 2 g/kg after fasting for 16 h. For insulin tolerance test (ITT), mice that had fasted for 6 h were injected intraperitoneally with human insulin at a dosage of 0.5 U/kg. Blood glucose concentrations were measured at 0, 15, 30, 45, and 60 min after injection by glucometer (One Touch Ultra, LifeScan Inc., Milpitas, CA).

### H&E staining and Sirius red staining

Pieces of iWAT and eWAT were fixed with 4% PBS buffered paraformaldehyde for 24 h at room temperature; then, they were subjected sequentially to dehydration in a 50%, 75%, 85%, 95% and 100% alcohol gradient for 1 h, before being made transparent in xylene and paraffin-embedded. Samples were cut into 5-μm sections. The sections were dried at 65 °C for 2 h and immersed in xylene to remove paraffin, which was followed by alcohol gradient rehydration and staining with a hematoxylin-eosin kit according to the instruction manual. For Sirius red staining, the slides were immersed in hematoxylin solution for 8 min, then soaked in Sirius red solution for 1 h, rinsed with acidified water for 3 times, and visualized on a Leica DM4B microscope with bright-field.

### *In vitro* adipogenesis

BMP4 (100 ng/mL), SB431542 (10 μM), and TGFβ1 (5 ng/ml) treatments were started when the initial confluence reached 50% and lasted for three days. Confluent cells were cultured for additional two days and harvested for subsequent analysis of preadipocyte determination factors. For white adipocyte differentiation of C3H10T1/2, 3T3-L1 and primary WAT SVFs, confluent cells were cultured for additional two days and induced by treatment with an MDI cocktail (0.5 mM isobutylmethylxanthine, 1 mM dexamethasone, and 10 μg/mL insulin) for 2 days. After 2 days, the cocktail was removed and replaced by 10 μg/mL insulin for another 2 days. Then, the cells were maintained in general growth media until harvest. For white adipocyte differentiation of nonadipogenic lineages, confluent cells were induced by treatment with a cocktail (0.5 mM isobutylmethylxanthine, 1 mM dexamethasone, 10 μg/mL insulin, and 0.5 μM rosiglitazone) for 2 days and then were treated with maintenance media containing high-glucose DMEM with 10% FBS and 10 μg/mL insulin. The maintenance media was changed every day until harvest.

### Immunofluorescence

Cell slides or glass bottom culture dishes (NEST biotechnology, China) were coated with rat tail collagen or poly-L-lysine to enhance cell adhesion before cell seeding. For immunofluorescence, cells were fixed with ice-cold 100% methanol for 15 min at -20 °C, washed with PBS 3 times at room temperature, and blocked in blocking buffer (PBS containing 5% FBS and 0.3% Triton X-100) for 1 h. Cells were incubated with primary antibodies overnight at 4 °C and then incubated with fluorescent dye-attached secondary antibodies for 1 h at room temperature in the dark. DAPI was used to visualize nuclei. Image acquisition and analysis were mainly performed with a Leica SP8 confocal microscope. For colocalization imaging, cells cotransfected with *mCherry-β-catenin*, *pLV-Flag-Lef1* and *pLV-EF1A-Sox4* plasmids were cultured for 48 h on poly-L-lysine coated high-precision cover glass. Then, the anti-FLAG antibodies and DAPI were used for immunostaining. SOX4 and β-Catenin were observed by coupled with GFP and mCherry fluorophores, respectively. Image acquisition was performed with Leica SP8 microscopy in the Core Facility of Biomedical of Xiamen University, and the image processing and analysis were realized by using image J.

### Isolation of SVFs and adipocytes, DNA quantification and flow cytometry

Excised subcutaneous white adipose tissues were digested in digestion solution (3 mg/mL type II collagenase, HBSS, 3% BSA) for 45 min at 37 °C. SVFs and mature adipocytes were separated from the adipose tissues by centrifugation at 500 g for 5 min. The suspended adipocytes and the precipitated SVFs were collected and lysed by TRIzol for subsequent RNA extraction and qPCR analysis. For DNA quantification, the suspended adipocytes were lysed by TNES (50 Mm Tris, 100 mM EDTA, 0.4 M NaCl, 5% SDS) and digested by protease K (0.1 mg/mL), followed by DNA purification and quantitative steps. For flow cytometry, isolated SVFs were washed with PBS and then were resuspended in erythrocyte lysis buffer (154 mM $NH_4Cl$, 10 mM $KHCO_3$, 0.1 mM EDTA) for 10 min to remove erythrocytes. The SVFs were sequentially filtered with

70- and 40-μm filters and blocked by blocking buffer (PBS containing 3% BSA) for 20 min followed by staining with appropriate antibodies for 30 min. After that, the sample were centrifuged and washed for 2 times and used for flow cytometry analysis by BD LSRFortessa or fluorescence-activated cell sorting by BD Aria III. The image processing and data analysis were realized by using FlowJo.

### Oil Red O staining and Nile Red staining

Cells were rinsed with PBS twice, fixed in 4% PBS-buffered paraformaldehyde for 20 min at room temperature and then washed with PBS. For Oil Red O staining, a 0.35% (W/V) Oil Red O stock solution (dissolved in isopropanol) was prepared in advance. Oil Red O working solution was prepared by mixing three parts of the stock solution with two parts of water and then centrifuging at 13000 rpm for 5 min at room temperature to remove undissolved particles. Cells were stained with the working solution for 10 min at room temperature and then were subjected to microscopic examination and image capture. For Nile Red staining, fixed cells were stained in working solution (3% BSA-PBS solution, 0.2 μg/mL Nile red, 5 μg/mL DAPI) for 10 min at 22 °C in the dark. The cells were rinsed with PBS to remove extra solution and then were photographed. All experiments were performed in triplicate.

### Chromatin immunoprecipitation assay (ChIP)

C3H10T1/2 cells were infected with pLKO.1-control, pLKO.1-Lef1-1 and pLKO.1-Lef1-2 lentivirus, respectively, and cultured until post-confluent. A total of $10^7$ cells for each group were cross-linked with 1% formaldehyde for 15 min, and the crosslinking was stopped by the addition of 0.125 M glycine for 5 min at room temperature. After two washes with cold PBS buffer containing 1 mM PMSF, cells were collected and lysed by SDS lysis buffer (1% SDS containing 10 mM EDTA, 50 mM Tris-HCl pH 8.0, 1 mM PMSF and 1 mM cocktail) for 10 min on ice. Cell lysates were sonicated under appropriate conditions to obtain 200-1000 bp DNA fragments. After centrifugation, the supernatant was diluted to a volume of 2 mL in dilution buffer and then were divided into two equal parts and incubated with IgG or Sox4 antibodies overnight at 4 °C. Protein A/G magnetic beads (70 μL) were added to each group and incubated for an additional 1 h at 4 °C with rotation. The magnetic beads were washed sequentially in low salt immune complex wash buffer, high salt immune complex wash buffer, and LiCl immune complex wash buffer for 5 min with rotation at 4 °C. Then, the beads were washed twice in TE buffer and extracted twice with freshly prepared elution buffer (1% SDS and 0.1 M NaHCO3). Subsequently, 5 M NaCl was added to the mixture at a final concentration of 0.2 M and incubated overnight at 65 °C to reverse formaldehyde cross-linking. For the removal of residual protein, samples were incubated with proteinase K for 1 h at 37 °C. The DNA fragments were purified and analyzed by qPCR using the specific primers listed in Table S1. This experiment was performed in triplicate.

### Co-immunoprecipitation (CoIP)

For endogenous immunoprecipitation experiments, cells were washed with PBS and lysed in IP lysis buffer containing cocktail and PMSF for 30 min at 4 °C. Then the lysates were sonicated briefly and centrifuged. The supernatants were precleared by treatment with magnetic protein A/G beads for 1 h at 4 °C while rotating. Appropriate antibodies were added to the precleared samples and incubated overnight at 4 °C. Then, the preblocked magnetic beads were added for an additional 1 h at 4 °C while rotating. Next, the beads were rinsed three times with IP lysis buffer and subjected to SDS-PAGE for subsequent analysis with appropriate antibodies. For semi-exogenous immunoprecipitation experiments, *Flag-Lef1* plasmid was transfected into Control or SOX4-deficient MSCs. After 48 h, these cells were collected, lysed, sonicated, and centrifuged. The supernatants were collected and precleared, and then the immunoprecipitation was performed by using magnetic beads coupled with β-Catenin antibodies. After 6 h, the precipitates were washed for 3 times and boiled for 10 min at 100 °C in 40 μL lysis buffer. The supernatants were obtained after brief centrifugation and used for Western blot analysis.

### GST pull-down

For construction of *GST-Sox4* and *GST-β-catenin* plasmids, the CDS sequence of mouse *Sox4* or *β-catenin* was cloned into pGEX-4T3 vector. For construction of *His-Sox4* and *His-Lef1* plasmids, the CDS sequence of mouse *Sox4* or *Lef1* was cloned into *pET-21b* vector. The fusion proteins were expressed in the *E. coli* strain BL21. The cells were lysed by sonication in lysis buffer (PBS, 1.5% Triton X-100, 2% β-mercaptoethanol, and 1mM PMSF). The lysates were incubated with glutathione-seph arose beads by rotating at 4°C for 40 min. The beads were pelleted by centrifugation and washed with lysis buffer for 3 times. His-fusion protein lysates were prepared and then incubated with the resin-bound proteins by rotating at 4°C for 3 h. The

samples were washed 3 times with lysis buffer and analyzed by western blotting using appropriate antibodies.

### Luciferase reporter assay

The luciferase reporter, β-galactosidase (β-gal), and other required plasmids were cotransfected into C3H10T1/2 MSCs by using DNA Transfectin 3000. 48 h after transfection, the cells were harvested and lysed in Luc-lysis buffer (1 M Tris PH7.4, 10% TritonX-100, 1 mM DTT, cocktail and PMSF), which was followed by centrifugation. The supernatants were used for luciferase and β-gal activity measurements. To correct errors caused by transfection efficiency, the luciferase activity was normalized to the corresponding β-gal activity. All experiments were performed in triplicate.

### Quantitative real-time PCR (qPCR) and western blot

Total RNA was extracted from cells or tissues with Trizol (Invitrogen), and a 5× All in One kit was used for first-strand cDNA synthesis. UltraSYBR Mixture and PCR machine (Bio-Rad) were used for the qPCR experiments. Primer sequences are listed in Table S2. All experiments were performed in triplicate. For Western blot analysis, cells or tissues were lysed in 2% SDS lysis buffer (50 mM Tris·HCl, pH 6.8, and 2% SDS) supplemented with proteinase inhibitor cocktail and PMSF. Lysates were centrifuged at 1,3000 g for 10 min at 4 °C, and the protein concentrations of supernatants were quantified by BCA assay kit. Samples were separated by SDS-PAGE and transferred to PVDF membranes. The membranes were sequentially incubated in blocking buffer (TBST containing 5% BSA) for 60 min at room temperature, primary antibodies overnight at 4 °C, secondary antibodies for 1 h and subjected to chemiluminescence imaging. All the experiments were repeated three or more times.

### Plasmids, production of lentivirus and lentivirus-mediated gene transfer

For construction of knockdown lentiviral plasmids, the shRNA sequences of *Sox4*, Lef1, *Tcf1*, *Tcf3*, and *Tcf4*, which are listed in Table S3, were cloned into a *pLKO.1* lentiviral vector. For overexpression of the mouse Sox4 gene, the CDS sequence was cloned into a *pLV-EF1A-puro* lentiviral vector, *pMSCV-puro* retroviral vector or *pLV-N-Flag-vector*. For the overexpression of the *Lef1* gene, the CDS was cloned into a *pLV-CS2.0* lentiviral vector. For the overexpression of the *β-catenin* gene, the CDS (S33Y mutant) was cloned into a *pLV-HA-vector* or *mCherry* vector. Lentiviruses were generated by cotransfecting target plasmids with the helper plasmids *pVSV-G* and *pHR* into 293T cells using polyethylenimine or turbofect transfection reagent. For lentivirus-mediated gene transfer in C3H10T1/2 MSCs or 3T3-L1 preadipocytes, the lentivirus was collected and concentrated using centrifugal filter units before being used to infect the target cells. The initial confluence of the target cells was 30%-50%. For construction of luciferase reporters, the gene sequences of *Lef1*, *Axin2*, and *Ccnd1* containing the adjacent LEF1 and SOX4 binding sites were cloned into a PGL4.26 promoter-less luciferase reporter cassette. The mutant luciferase reporter was constructed by truncating the Sox4 binding element A/T A/T CAAA T/G in *Lef1-Luc* reporter plasmid. The primers used for construction of luciferase reporters are list in Table S4.

## QUANTIFICATION AND STATISTICAL ANALYSIS

Statistical comparisons were determined by unpaired two-tailed Student's t test. Normal distribution was assumed. All statistical tests were performed with GraphPad Prism 8 software. The differences were considered statistically significant at $P < 0.05$ and reported as follows (*$P < 0.05$, **$P < 0.01$, ***$P < 0.001$; ****$P < 0.0001$; *ns*, no significance). Investigators were not blinded to group allocation during experiments.